CHAPTER II

THEORY AND LITERATURE REVIEWS

2.1 Dimerization of fatty acid [2]

Dimerized fatty acids, along with fatty esters, amines and amine derivatives, amides, alcohols, and metallic stearates, are important commercial fatty ester derivatives. Dimer acids is the general term applied to products obtained by the intermolecular reaction of two or more molecules of unsaturated fatty acids or unsaturated fatty acid esters. For the most part, the unsaturated fatty acids used commercially in manufacture are those which have 18-carbon atoms such as oleic. As a result, the finished products are mostly 36-carbon entities Figure 2.1.

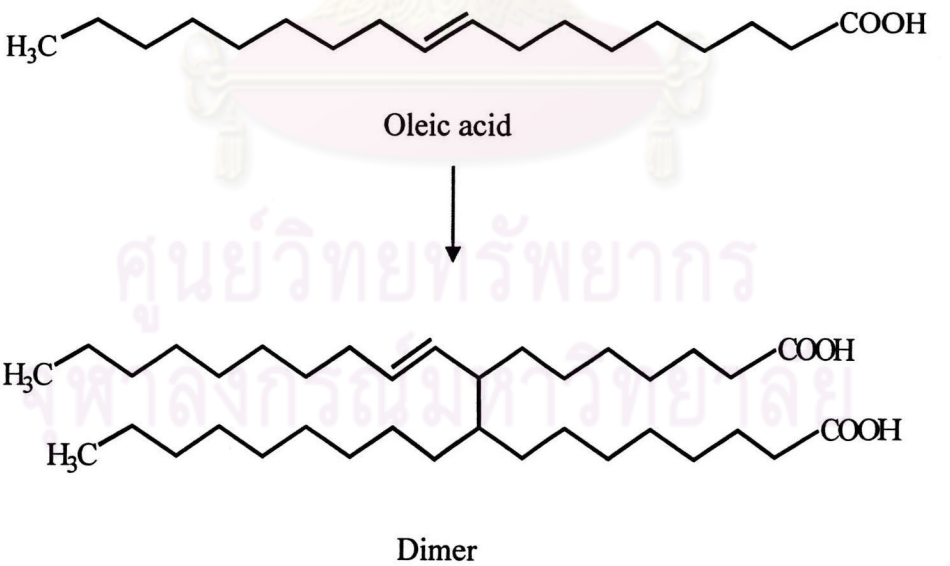

Figure 2.1 Dimer of oleic acid

On commercial products, the degree of fractionation determines the level of trimer and higher oligomers, as well as the trace percentages of unpolymerized, or structurally altered, 18-carbon, monocarboxylic acids. There have been a variety of structures suggested for dimer acids. Dimerization of unsaturated fatty acids has been claimed to lead to cyclic structures by a Diels-Alder reaction, and to linear dimmers and higher oligomers by a free-radical route involving hydrogen transfer, particularly in the presence of oxygen. Clay-catalyzed dimerization of unsaturated fatty acids appears to be a carbonium ion reaction involving double bond isomerization, acid catalysis, hydrogen transfer, and chain branching. Some idealized possible structures for dimer acid methyl esters are shown in Figure 2.2.

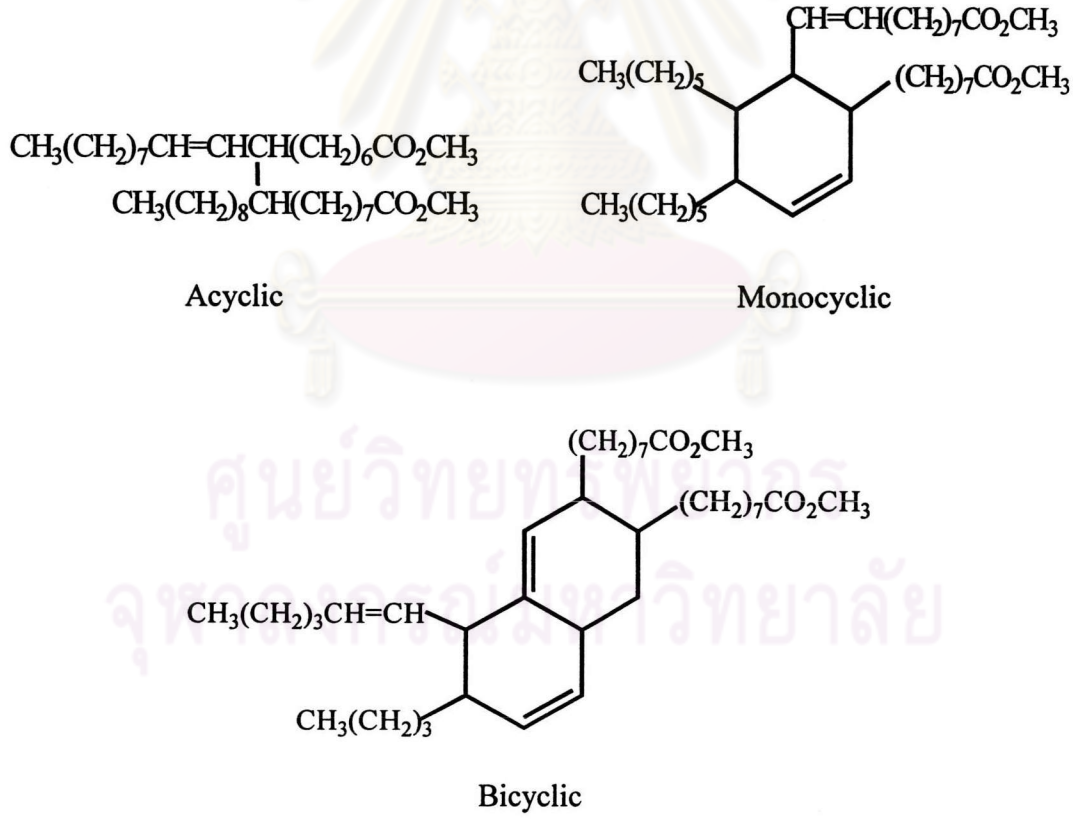

Figure 2.2 Some possible structures of dimer from fatty acid methyl ester.

2.2 Clay mineral

2.2.1 Introduction [3]

Clay minerals have long been recognized as efficient material for the promotion of many organic reactions. They are highly versatile, affording both industrial and laboratory catalysts with excellent product-, regio- and stereo-selectivity. Clay catalysts have distinct advantages over homogenous catalyst as the work- up of the reaction mixture is often very simple, i.e. the clay is removed by filtration. Clays are powerful adsorbents with extremely high surface areas, especially when acid activated, and industrially, they are used in such diverse applications as the co-reactant for carbonless copying paper development and the decolorizing of vegetable oils.

The term "bleaching earths" refers to clays that their naturals states or after chemical or physical activations, have the capacity to adsorb coloring matters from oil. Bleaching earths are finely crystalline silicates of aluminum and/or magnesium with variable amounts of lime, alkalis and irons with a large proportion of water of hydration. Bleaching clays are often classified as fuller's earths and Bentonites according to their inherent properties. The geologically term "Bentonites" refer to any devitrification of volcanic ash. Mineralogically, bentonites are 75 percent or more of montmorillonites with fragment of kaolinite, illite felspar and traces of other minerals. The best known property of bleaching earth is its high adsorption capacity, with can be enhanced by acid treatment.

Bleaching clays in powder or granular form were used for the refining of petroleum products using two main processes : contact and percolation. In the contact

process, recovered oil, paraffin wax or liquid paraffin is previously treated with sulfuric acid to remove acid tar, and after its decantation the bleaching earth is added. In the percolation process, the solvent to be treated is passed through a tower containing a bed of bleaching clay granules.

2.2.2 The structure of clay minerals [4]

Clay minerals are the most abundant sedimentary mineral group. They predominate in the colloidal fractions of soils, sediments, rocks and waters and are classified as phyllosilicates or hydrous aluminosilicates. In geology the word clay is used in two ways: firstly as a rock classification which generally implies an earthy, fine- grained mater material that develops plasticity on mixing a limited amount water. Secondly, it is used as a particle size term, which describes clay as materials which have particle sizes <4 μm, although the modern tendency is to define clays as having partice sizes <2 μm as factions of this size generally give the very pure mineral. Clay minerals are characterized by an extremely fine particulate construction and by a composition which is based primarily on oxygen and hydrated silicates of aluminum, iron and magnesium. They have been shown by X-ray diffraction studies to be crystalline, even in their finest particles, although the presence of traces of amorphous materials have been verified in some clay sample. Most of the important clay minerals are made up of combinations of two basic types of layers, the first consists of sheet of $[SiO_4]^{4-}$ tetrahedra arranged in hexagonal ring sub-units, show in Figure 2.3. Each silica ring is combined with the two adjacent ring so as to form another 12-membered ring.

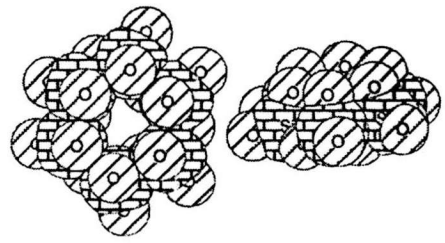

Figure 2.3 Silica sub-units of the tetrahedral sheets.

The second type of layer is usually composed of ether gibbsite [$Al_2(OH)_6$] or brucite [$Mg_3(OH)_6$] units which form octahedrally coordinated sheets, with the octahedral arranged so that each oxygen atom is shared with two neighboring metal atoms, show in Figure 2.4.

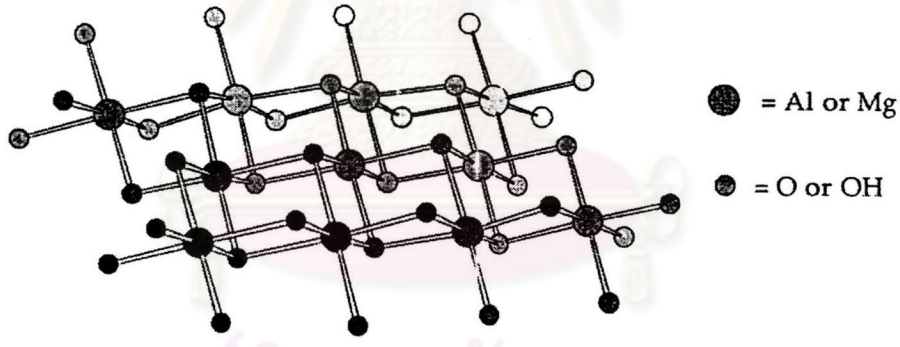

Figure 2.4 The arrangement of atoms in a dioctahedral layer.

There are two dominant patterns of combining the layers. The first has alternating tetrahedral and octahedral sheets and is describes as a T:O or 1:1 arrangement. This group includes kaolinite ($Al_4Si_4O_{10}(OH)_8$) – the main constituent of china clay – and crystolite ($Mg_4Si_4O_{10}(OH)_8$). The main bonding forces between layers are hydrogen bonds between –OH on one layer and a bridging –O- on the next.

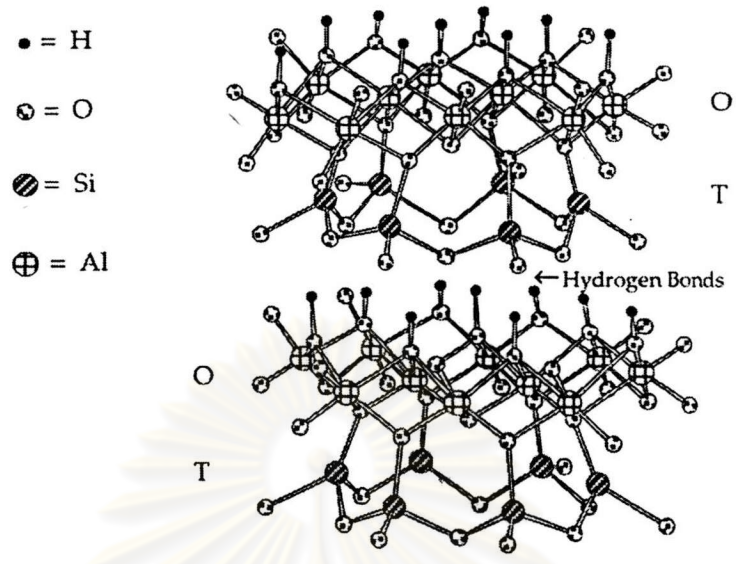

Figure 2.5 The idealised structure of kaolinite.

The second, and perhaps chemically more important type, has repeating units of tetrahedral:octahedral:tetrahedral layers and is described as a T:O:T or 2:1 arrangement .If the octahedral layer consists of M^{2+} cations then all of the octahedral sites must be occupied to maintain electrical neutrality.However,if an M^{3+} cation is used then only 2/3 of the octahedral sites need be occupied to maintain neutrality. The former mineral type is thus known as trioctahedral and the latter as dioctahedral.

Illite $(K_{1.6}Si_{6.4}Al_{5.6}O_{20}(OH)_4) + (H_2O)_x$

Montmorillonite $(Na_{0.6}Al_{3.4}Mg_{0.6}Si_8O_{20}(OH)_4) + (H_2O)_x$

The formulae given here are idealised general formulae and large variations in composition are encountered within each sub-group of minerals; for instance most montmorillonites have at least a few percent of Fe^{3+} cations replacing the octahedral Al^{3+} cations and Ca^{2+} cations often replace the interlayer Na^+ One of the most useful groups of clays is the smectite (swelling) clays, this group includes montmorillonite and hectorite. Montmorillonite is the main constituent of bentonites and fuller's Earth

which are noted for their excellent swelling properties when wetted. The most important bentonite clay is the montmorillonite group of minerals. Figure 2.6, at the atomic level, montmorillonite possesses the layered sheet structural that is typical of most minerals. Each sheet consists of a three-layer sandwich of ions in octahedral form. The central layer consists of aluminium ions surrounded by oxygen ions in tetrahedral form.

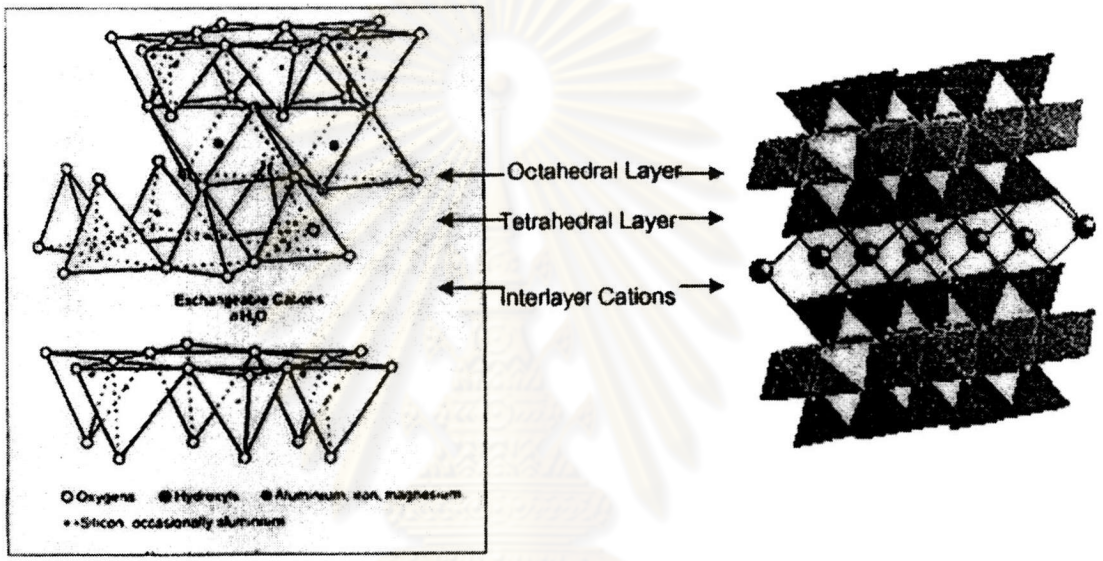

Figure 2.6 Structure of montmorillonite.

2.2.3 Ion exchange of clays

Clay minerals have the property of sorbing certain anions and cations and retaining these in an exchangeable state; i.e., they are exchangeablefor other anions or cations by treatment with such ions in a water solution (the exchange reaction also takes place sometimes in a nonaqueous environment). The exchange reaction is stoichiometric. The exchangeable ions are held around the outside of the silica-alumina clay mineral structural units, and the exchange reaction generally does not affect the structure of the silica-alumina packet .

More information is available regarding cation exchange than anion exchange. In clay minerals the common exchangeable cations are calcium, magnesium, hydrogen, potassium,ammonium, and sodium, frequently in about that order of general relative abundance. The common anions in clay minerals are sulfate, chlorine, phosphate, and nitrate. The general relative abundance of the anions is not yet known. The property of ion exchange is of great fundamental and practical importance in the investigation of the clay materials. In the application of clay mineralogy it is important because the nature of the exchangeable ion may influence substantially the physical properties of the material . Thus, a clay material carrying sodium frequently has very different plastic properties than material the same in every way except that calcium is exchangeable cation.

2.2.3.1 Cation exchange clays

To a greater or lesser degree, many clays have the ability to adsorb and exchange cation form solution and it is this cation 'storage' that makes clays such an important component of many soils. A typical montmorillonite can exchange over 100 millimoles of M^+ cations per 100 g of clay, whilst a kaolinite only adsorbs a few tens of millimoles. The ideal structures of the clay minerats depicted above are deviated from in a number of ways which introduce charge imbalances into the structure. The main causes of these charge imbalances are isomorphous exchange of Al^{3+} cations for Si^{4+} in the tetrahedral layers (e.g. in true montmorillonites), and of Li^+ for Mg^{2+} or Mg^{2+} for Al^{3+} cation in the octahedral layer and crystal defects (e.g. in true kaolinites), usually at the crystallite edge. Natural minerals will usually combine each of these types of exchange sites. The layers therefore have an overall negative

charge which is balanced by adsorption of metal cations into the interlayer region of the clay mineral in Figure 2.7

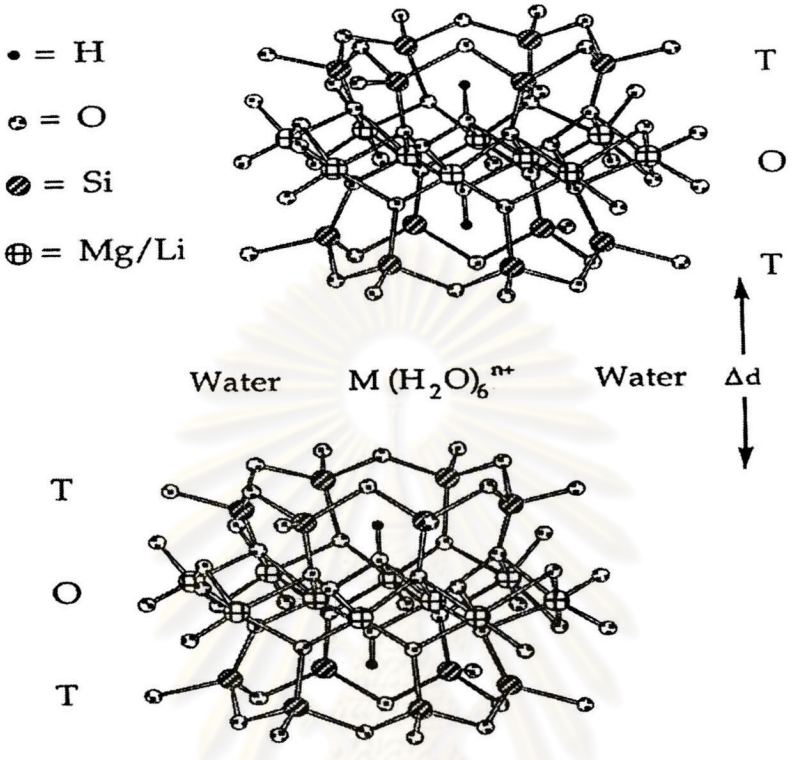

Figure 2.7 The idealised structure of a trioctahedral smectite clay showing the interlayer aqueous metal cations.

A typical montmorillonite will have Na^+ , Ca^{2+} or Mg^{2+} cations in the interlayer space. These cations are hydrated, usually hexa(aqua), and the remainder of the interlayer is filled by a variable amount of water which can swell the clay. The interlayer cations are much less strongly bound than the layer cations and will thus easily exchange with cations from an aqueous solution . Very small cations such as Li^+ initially occupy the inter layer region, but they can migrate on heating through the hexagonal cavities in the silica layer to occupy unfilled octahedral sites. This decreases the ability of the mineral to adsorb cations.

The position in which these adsorbed cations reside depends upon the hydration of the clay, the cation and whether edge or layer charges are involved. Na^+ and Ca^{2+} cations sit in the hexagonal cavities of the silica in dry montmorillonite, but they move into the interlayer region as the clay is hydrated. In contrast, kaolinite, whose charge imbalance is due mainly to edge defects , adsorbs the metal ions at the edges of the particles. Excess water can separate the metal cation from the surface by imposition of extra aquation spheres.

When a solution of a metal cation is used to exchange the interlayer cations of a clay. It has been observed that the smaller the size of the exchange cation and the higher the charge on the more powerful that cation is at replacing the interlayer exchangeable cations. Similarly the ease of replacement of interlayer cations follows the reverse trend. Thus the following series can be constructed:

$$M^+ << M^{2+} < H_3O^+ = K^+ = NH_4{}^+ < M^{3+} < M^{4+}$$

Increasing Exchange Power

(Decreasing Ease of Exchange)

Figure 2.8 The exchange properties of cations with clays.

There are three causes of cation-exchange capacity of the clay minerals:

1. Broken bonds around the edges of the silica-alumina units would give rise to unstisfied charges which ciuld be balanced by adsorbed cations. The number of broken bonds, hence the exchange capacity due to this cause, would increase as the particle size decreased. in kaolinite mineral broken bonds is the major cause of

exchange capacity. Montmorillonites broken bonds is respinsible for a relativeky small portion (20 percent) of the cation-exchange capacity.

2. Substitutions within the lattice of trivalent aluminum for quadriva-lent silicon in the tetrahedral sheet and of ions of lower valence, per-ticularly magnesium, for trivalent aluminum in the octahedral sheet result in unbalanced charges in the structural units of some of the clay minerals. In montmorillonite substitutions within the lattice cause about 80 per cent of the total cation-exchange capacity.

3. The hydrogen of exposed hydroxyls may be replaced by a cation which would be exchangeable. Some hydroxyl groups would be exposed around the broken edges of all the clay minerals, and cation exchange due to broken bonds would, in part at least, be replacement of the hydrogens. There is considerable doubt that this factor is a substantial cause of the cation-exchange reaction since it seems quite certain that the hydrogen of the hydroxyl would not normally be replaceable under the conditions of the exchange reaction.

In the clay minerals in which cation exchange results from broken bonds, the exchangeble cations are held around the edges of the flakes and elongate units. In the clay minerals in which the exchange reaction is due to lattice substitutions, the cations are held mostly on the basal-plane surfaces.

Therefore, in kaolin minerals, some compounds can intercalate directly into kaolinite, some can be introduced by displacement of a previously intercalated. Some compounds cannot intercalate into the basal spacing of kaolinite but are adsorbed on the edges of faces of the clay particles. Little systematic work appears to have been done to explain why kaolin minerals spontaneously expand in some polar organic compounds, but not in others.

In montmorillonite, organic compounds are adsorbed in the interlayer space of the clay. Desorption investigations indicated that the cation adsorbed on the edge of the kaolinite clay particles are not held as strong as those bound within the clay lattice of the montmorillonite. The mechanism of organic adsorption on clay mineral is depicted according to the following exchange reaction.

$$(\text{Organic cation}^{2+}) + (2\text{Na} - \text{Clay}) \longrightarrow (\text{Organic cation} - \text{Clay}) + 2\,(\text{Na}^{+})$$

2.2.3.2 Anion exchange clays

A series of clay minerals of lesser importance, whose charge imbalance or layer substitution pattern has given them positively charge layers, are known. Such minerals as hydrotalcite ($Mg_{4.5}AlO_{7.5}$) and xonotlite ($Ca_6Si_6O_{17}(OH)_2$) can be used as solid 'carriers' of hydroxy and *t*-butoxy anions, respectively.

2.2.4 Acidity of Clays

Several measurement of the acidity of clay surfaces have been carried out using surface conductivity, nuclear magnetic resonance and Hammett indicator methods. These experiments show that the effective pH of water at the mineral surface is usually between 1.5 and 3; which is 4 to 5 units more acidic than of bulk water. Clay minerals show both Bronsted and Lewis acidity. Structural and environmental factors govern the degree to which is present and normally one type predominates for a given set conditions.

A further source of acidity is associated with the –OH groups of the octahedral layer which protrude into the interlayer region via the holes of the ring. The incidence of these protons may be increased by preparing a 'proton-exchanged' clay. This is achieved either a simply exchanging the clay with dilute acid, or less destructively to exchanging the clay with ammonium ions and calcining at 200-300 ^{0}C to expel ammonia. The exchanged proton can migrate into vacancies on the octahedral layer of dioctahedral clays where they protonate bridging oxygen.

2.2.5 Acid Activation of Clays

Smectite clays are often treated with strong mineral acid (acid activated) to give materials of very high surface area which have excellent activity as adsorbents and catalysts. The application of acid-activated clays as a developer for carbonless coying paper, requires a high brightness of the material.Acid activation improves the brightness mainly by removal of structural Fe^{3+} cations which cause the clay to be a grey or yellow colour.

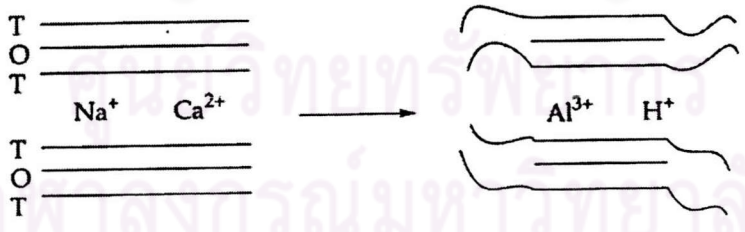

Figure 2.9 Diagrammatic representation of the effects of acid activation.

The acid activation process is often quite severe (>5 mol dm^{-3} hot mineral acid for several hours) and destroys much of the bentonite layer structure as it

removes iron, aluminium and magnesium from the octahedral layer. Scanning electron microscopy shows that the edges of the clay partiucles become very disordered and consist mostly of 'floppy' silica sheets. The exchangeable cations are replaced mainly by Al^{3+} and H^{+} cations.

Acid activation enhances the natural ability of montmorillonites to adsorb polar molecules. The naturally occurring substitution of magnesium (+2) ions for aluminium (+3) ions in certain clay deposits leaves a negative charge, which thus requires a positive charge go achieve electroneutrality. This positive charge is supplied by cations, such as sodium (+1) or calcium (+2), which are located between the sheets.

Clay activation step by acid attack [5]

1. Acid attacks octahedral layer

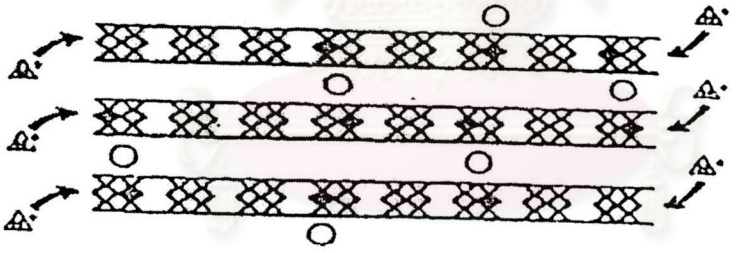

2. Structure disrupted surface area increases

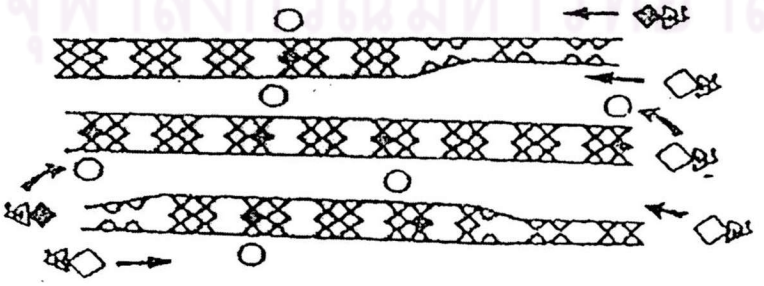

3. Acid cations released from structure exchanged for cations

4. Acid activated clay with acid cations in exchange sites

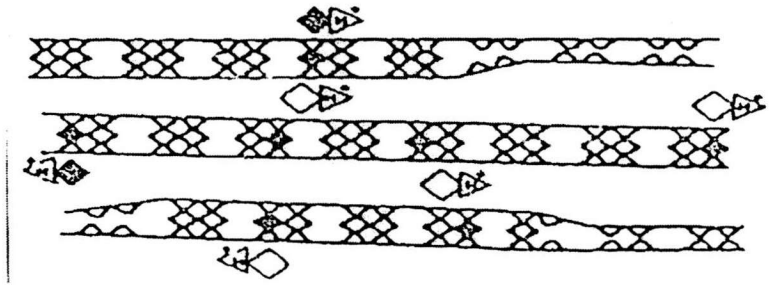

A well – controlled process has been developed to activate montmorillonites, exploiting the natural characteristics of its structure. The principle is to render soluble the structure cations in the octahedral layer, thus opening up the structure and increasing surface area. This allows more acidic (active) cations released from the octahedral layer to replace the less acidic cations originally present in the space between the sheets, thus increasing its characteristic acidic adsorption and catalytic nature. There is considerable evidence that acidic (active) cations serve as the active sites in the activated clay. When a pigment molecule (polar impurity) approaches one of the active sites, a carbonium ion (organic cation) forms and replaces, or associates with, one of the active, acidic inorganic interlayer cations. Now anchored in place by electrostatic force, the captive pigment molecule can be removed from the system along with the clay by simple filtration.

2.2.6 Some clays in Thailand

2.2.6.1 Ball clay

The name "ball clay" is derived from an early custom in the United Kingdom of excavating clay by cutting it into one-cubic foot blocks, which eventually became rounded to form balls. "Plastic clay" is a term used to describe fine-grained,

highly plastic, principally kaolinitic sedimentary clays. However, the principal type of plastic clay, used in the whiteware industry because it fires to a white or near white colour, is called "ball clay".

They are found from many resources in Thailand, scattering from northern, middle to southern parts of the country. Northern ball clays are Lampang ball clay from Ban jae Korn and brown ball clay form Ban Mae Than which is the largest clay production area. Ball clays in the middle and eastern parts of Thailand are in Pracheanburi and Chantaburi Provinces. Southern ball clays were found in the areas of Amphur Nasarn, Viensah, Kanchanadith, Surat Thani Province and in Nakoronsithammarat Province at Amphur Chwang, Pipoon, Lansaka, Ron Phibun and Sichon. Ball clays of Thailand have high plasticity and fine grain size and often high content of organic material. Although the clay mineral is essentially kaolinite, it is much finer than that found in china clay, giving ball clays greater plasticity and dry-strength than china clays. They contain a greater quantity and variety of impurity than china clays. Iron and titanium impurities give the clays a fired colour which may vary from off white to dark brown depending on the amounts, of the clays. The advantages of ball clays are their high plasticity and dry-strength; their disadvantages are fired are fires colour and low refractoriness.

Additional, the clay mineral of the majority of ball clays is the disordered form of kaolinite and has a high cation exchange capacity (c.e.c.), of the order of 30-40 meq/ 100 g. Since, however, non-clay invariably present, ball clays as mined have a c.e.c. somewhat lower than this, the average being around 15 meq/ 100 g. organic matter makes a large contribution to the c.e.c. of ball clays.

High –quality ball clay can make up 30 percent of the body mix of wall tiles, vitreous china, sanitary ware, and insulator porcelain, and 5 to 25 percent of

earthenware and ordinary porcelain. Plastic clays of lower grade are used in heavy products such as pipe, brick, and tile. Ball clays are also used in refractories, as anti-caking agents in animal feedstuffs, and as fillers in rubber and plastics.

2.2.6.2 China clay

There are residual clays, and are essentially composed of the clay mineral kaolinite contaminated with silica, mica, feldspar and partly decompised feldspar, all from the rock which the clay was formed. They are found in Northen parts; Lampang, Changmai and southern parts: Ranong, Nakornsrithammarat.

China clay is much finer then the contaminating materials, and thus is relatively easily purified by sedimentation, giving a white clay which is also white burning due to its low content of colouring impurities, particularly iron and titanium compounds. Additional, china clays have a comparatively low cation exchange capacity, ranging from about 2 to 10 meq/100g, the chief exchangeable ions being H, Ca, Mg, Na and K. Large quantities of china clay are used is paper manufacture as well as in the ceramics industry.

2.2.6.3 Talcum

Talc is different form of hydrated magnesium silicate which has a composition varying between the limits :

$3MgO.\ 4SiO_2.\ H_2O$ and $4MgO.\ 5SiO_2.\ H_2O$

31.8% 63.5% 4.7% 33.5% 62.7% 3.8%

associated with impurities introducing alumina, iron, lime, alkalines and more water.

Talcum is secondary rock formed by various interactions of water together with magnesium salts on the primary rocks. Although there are a large number of deposits, workable sources of a pure product are not nearly so frequent as those of clay. The mineral of clay is white to light green, extremely soft and has a greasy feel. Where the mineral is laminated and very soft : it is termed talc ; impure varieties are known as soapstone. The more massive and relatively pure varieties are known as steatite.

The requirements for talc for steatite insulators (of which it is the major constituent) should be soft, substantially free from foliated, fibrous material and from gangue which makes dark spots when fired. The colour of the raw talc is of no importance, but should be white after heating to 1350 ^{0}C in an oxidising or neutral atmosphere. The desirable chemical composition as compared with the theoretical is :

Theoretical : $3MgO.\ 4SiO_2.\ H_2O$ (SiO_2 63.4%, MgO 31.9%, H_2O 4.7%)

Desired limits: SiO_2 not less than 60%, MgO not less than 30 %

Al_2O_3 not more than 2.5%, CaO not more than 1.0 %

Fe_2O_3 not more than 1.5%, Na2O+K2O not more than 0.4%

Loss on ignition not more than 6.0%

Acid soluble lime not more than 1.0%

The properties of talc are high melting point (1490 ^{0}C) , specific gravity 2.6-2.8, thermal conductivity (2.3-2.8)/360 c.g.s., specific heat 0.2-0.3 c.g.s. The main uses of talc is therefore those taking full advantage of the good electrical properties and thermal shock resistance, that is for electrical porcelain, saggers and kiln furniture for use up to 1250 ^{0}C and use as electrical insulators.

2.3 Fatty Acid Free Radical Autoxidation [6]

The susceptibility of unsaturated fatty acid to autoxidation varies according to the lability of their allylic hydrogens. The hydroperoxidation of unsaturated fatty acids has been reviewed in detail previously. This subject will only be summarized here as a basis for further discussion of autoxidation of unsaturated fats and decomposition of hydroperoxides. The most accepted mechanism of autoxidation involves hydrogen abstraction on carbon-8 and carbon-11 with formation of two allylic radicals. These radical intermediates react with oxygen at the end carbons to produce a mixture of 8-, 9-, 10-, and 11-allylic hydroperoxides. Quantitative studies of isometric hydroperoxides showed that only for oleate, the 8- and 11-hydroperoxides were slightly but consistently higher than the 9- and 10-hydroperoxides (Figure 2.10 and Figure 2.11).

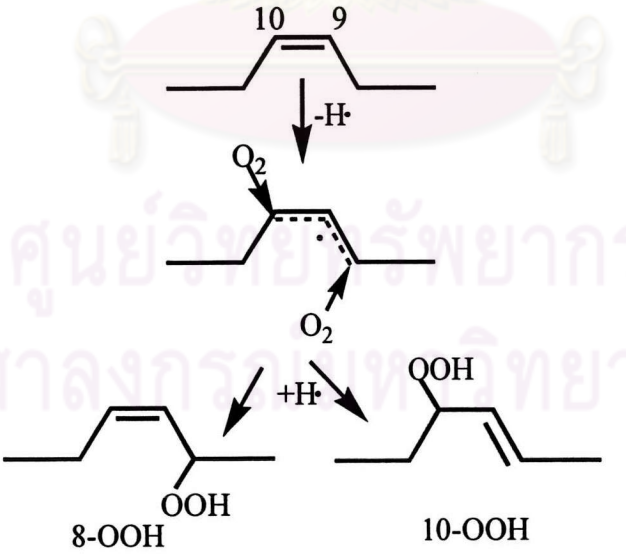

Figure 2.10 Mechanism of oleate autoxidation 8-OOH and 10-OOH

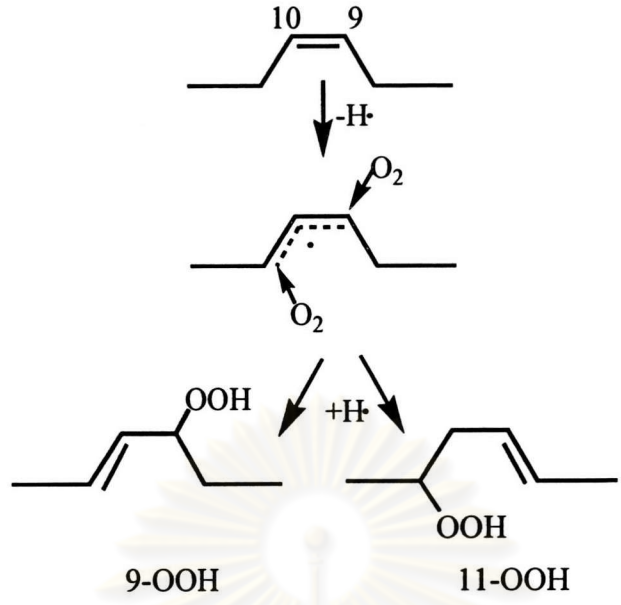

Figure 2.11 Mechanism of oleate autoxidation 9-OOH and 11-OOH

2.4 Decomposition of Hydroperoxides

A variety of volatile and nonvolatile secondary products are formed hydroperoxides when lipid oxidation is carried out to high conversion or at elevated temperatures. A very complicated set of reaction paths has been recognized for hydroperoxide decomposition. Although there is extensive literature on the nature of secondary lipid oxidation reactions, the decomposition products are so complex that much of these studies can be regarded as only qualitative accounts. In the following reaction sequence, the first step of the decomposition of an unsaturated hydroperoxide is the hemolytic cleavage of the oxygen-oxygen bond to yield an alkoxy and hydroxy radical .

2.5 Free radical dissociation [7]

In order to locate points of scission and decomposition in the products of autoxidation reaction, it may be necessary to determine the possible weaker points. Table 2.2 records the bond strengths between different atoms in such molecules, as collected from different reliable sources. The C–H bond adjacent to a double bond is labile; its value of dissociation falls off due to resonance stabilization during the activated stage in autoxidation reaction and further decrease while it is in transition to the stable state of a free radical. The C–H bond strength is very low in the natural linoleate system, and so the induction period of autoxidation is considerably low and sometimes undetectable. The values for O–O, O–H and C–O bond will indicate the point of scission of –CH OOH. The O–O bond strength is always low, and its easy dissociation has been proven by various workers by identification of the products. One bond in the C=C bond is easy to break, but the resulting product is not stabilized; rather it is unstable. The weak C–C bond between carbon α and β to the double bond may bring forth some clues to the scission products. The knowledge of the bond strength and its dissociation energy will also indicate the importance of the applications of tracers to the autoxidation reactions. Evidently deuterium in the positions of labile hydrogen may indirectly determine the point of activity in a molecule by decreasing by virtue of its isotopic effect, such lability and consequently the reactivity. Heavy oxygen may play the same role in scission of the O–O bond.

Table 2.1 Free radical dissociation

Bond	Nature	Bond strength
		(K-Cal)
C–H	Ordinary as in CH_4 etc	99-100
C–H	Hydrocarbons	p>s>t
C–H	Ethylene	91
C–H	Labile adjacent to one double bond	80
C–H	Same as above but activated due to resonance	<64
C–H	Doubly flanked by double bond	<<64
C–H	Adjacent to conjugated double bonds	>64
O–O	In hydrogen peroxide (HO-OH)	64
O–O	In hydroperoxide (CO-OC)	66
O–O	Di-alkyl peroxide (CO-OC)	>66
O–O	Di-acly peroxide	<64
O=O	In oxygen molecule	118
O–C	In peroxide	87
O=C	In aldehyde	174
O=C	In ketone	174
O–H	In H–O–H	110
O–H	In $H–O_2–H$	100
O–H	In $RO_2–H$	>100
–C=C–	Carbon to carbon double bond	145
–C=C–	–C–C—(one bond fission)	64
–C–C–	General	81
–C…C–C=O–	Bond between C-atoms, alpha and beta to double bond	<81

2.6 A Computer Program for Transition Metal Catalyzed Liquid Phase Autoxidation [8]

Algebraic analyses based upon steady-state approximations were employed to a limited extent in the previous discussions. This program has been applied to test the extent to which the mechanism outlined in reactions 1-13 is capable of reproducing the cobalt-catalyzed oxidation of tetralin in chlorobenzene solution at 65 ^{0}C. The rate constants used for reaction 1-15 and the source for each are presented in Table 2.3.

Table 2.2 Rate Constants (mol $L^{-1}s^{-1}$) Used for the Metal-Catalyzed Oxidation of Tetralin in Nonpolar Media at 62 ^{0}C.

Eq	Reaction	K(65 ^{0}C)
1	$Co^{2+} + ROOH \longrightarrow (ROOHCo)^{2+}$	40
2	$(ROOHCo)^{2+} \longrightarrow Co^{2+} + ROOH$	2×10^{-2}
3	$(ROOHCo)^{2+} \longrightarrow RO^{\cdot} + Co^{3+} + OH^{-}$	2×10^{-2}
4	$Co^{3+} + ROOH \longrightarrow (ROOHCo)^{3+}$	40
5	$(ROOHCo)^{3+} \longrightarrow Co^{3+} + ROOH$	2×10^{-2}
6	$(ROOHCo)^{3+} \longrightarrow RO_2^{\cdot} + Co^{2+} + H^{+}$	2×10^{-3}
7	$RO^{\cdot} + RH \longrightarrow ROH + R^{\cdot}$	1×10^{6}
8	$R^{\cdot} + O_2 \longrightarrow RO_2^{\cdot}$	3×10^{8}
9	$RO_2^{\cdot} + RH \longrightarrow ROOH + R^{\cdot}$	24
10	$RO_2^{\cdot} + RO_2^{\cdot} \longrightarrow$ Products	6.6×10^{6}
11	$RO_2^{\cdot} + Co^{2+} \longrightarrow Co^{3+}$ + Products	1×10^{5}
12	$R^{\cdot} + Co^{3+} \longrightarrow Co^{2+}$ + Products	5×10^{4}
13	$RO^{\cdot} + ROOH \longrightarrow ROH + RO_2^{\cdot}$	1×10^{7}

2.7 Literature reviews

The literature reports related to the dimerzation of methyl oleate by various methods, are the followings :

Koster *et al.* [1] described the relative importance of the various acid sites as well as structural and textural parameters of montmorillonite for the dimerization of oleic acid. It is shown that reaction in the interlamellar space dominates the oleic acid dimerization. The active site is the tetrahedral substitution site, and the influence of the type of interlayer cation on the activity of montmorillonite is explained in terms of its effect on the interlayer distance. Model catalysts with mesopores and tetrahedral substitution sites do not show any activity in oleic acid dimerization.

Leonard [2] studied clay-catalyzed and high temperature polymerization of unsaturated fatty acids, usually tall oil fatty acids. The products are high boiling, mobile to viscous liquids, Their most important chemical property is carboxyl multifunctionality, which allows conversion to high polymers, mostly polyamides in commercial practice.

Barrett *et al.* [9] presented process of dimerized fatty aids from monounsaturated fatty acids such as oleic acid, its isomers, erucic acid, its isomers, undecylenic acid and other monounsaturated fatty acids having a chain length of 11 to 22 carbon atoms. The method comprises heating a monounsaturated fatty acid, such as oleic acid, with crystalline clay mineral and water. A 36 carbon dicarboxylic dimerized acid is the product.

Lawrence *et al.* [10] presented method for polymerization of unsaturated fatty acids by heating unsaturated fatty acids in the presence of a particular neutral clay catalyst. The usual temperature range is from about 225 ^{0}C to about 270 ^{0}C for a period of about one to about 5 hours. Moisture is usually present in the reaction mixture in an amount of from about 2 to 5 percent by weight of the reaction mixture.

Kumar *et al.* [11] evaluated the surface acidity and porosity of bentonite clay on treating with sulfuric acid. It was observed that clay treated with 4 N sulfuric acid showed the maximum surface acidity. Acid strength distribution as measured by Benesi's technique of nonaqueous titration show acidity range mainly between H_0 +4.6 and +3.3. Nitrogen adsorption-desorption data indicated the transformation of pores from slit-shaped to spheroid inkbottle type as the acid concentration is increased from 1 to 8 N. X-ray diffraction and FTIR explained the observations in terms of structural modifications of clay on treatment with acid.

Neff *et al.* [12] studied the structures of dimers and oligomers produced by autoxidation of methyl linolenate and its purified oxidation products were investigated to obtain a better understanding of the mechanism of oxidative deterioration of unsaturated lipids. The dimers were separated by gel permeation chromatography, characterized by molecular weight determinations before and after sodium borohydride reduction, and analyzed by ultraviolet, infrared, ^{1}H NMR and fast atom bombardment mass spectrometry. Autoxidation of methyl linoleate monohydroperoxides at 40 ^{0}C produced dimmers that were peroxide- and ether/carbon linked.

Frankel *et al.* [13] deleloped a liquid partition chromatographic method was developed to isolate and determine hydroperoxides in autoxidized fatty acids or their methyl esters. By the use of benzene containing 2 to 4% methanol as the mobile solvent, the hydroperoxides were separated from unoxidized fatty acids or methyl esters and form secondary and polymeric decomposition products. In the analyses of oxidized fatty acids, diethyl ether was necessary in the elution of secondary decomposition products.

Falla [14] studied the alkydfilms to be polymers based on $C_{10}H_{18}O_3$ repeated units with carboxylic acid, aldehyde, or hydroxyl end groups. The results indicated that the polymerization of a long oil alkyd coating is accompanied by scission of the fatty acid chains to leave C9 residues attached to the polymer backbone in place of the C18 moieties. Such reactions can be expected to occur both during the initial drying and subsequent aging of the coating, and the loss of these C9 plasticizing components must have a significant effect on the physical properties of the alkyd film.

Miyashita [15] reported that the dimmers isolated from hydroperoxides aerated for 90 min could be separated into two fractions according to their polarities. The dimers were identified as octadecadienoate and oxygenated octadecenoate moieties crosslinked thought either ether or peroxy linkages across C-3 or C-13 positions. The oxygen-containing functional groups found in the dimers included hydroperoxy, hydroxy and oxo groups. The polar dimers had two of these groups per molecule, while the less polar dimers had one. The polar main constituents of dimers were linked through peroxy bridges and found to be similar to the dimers previously identified in autoxidized methyl linoleate.

CHAPTER III

EXPERIMENTAL

3.1 Materials and chemicals

1. Sulfuric Acid: Analytical grade; Merck
2. Phosphoric Acid: Analytical grade; Fluka
3. Acetone: Analytical grade; Lab-Scan
4. Methanol: Analytical grade; Merck
5. Dichloromethane: Analytical grade; Lab-Scan
6. Hexane: Analytical grade; Lab-Scan
7. Ethyl acetate: Analytical grade; Lab-Scan
8. Anhydrous Sodium Sulfate: Analytical grade; Merck
9. Sodium Hydrogen Carbonate: Analytical grade; Merck
10. Chloroform-D1: NMR spectroscopy grade; Merck
11. *tert*-Butyl hydroperoxide: Analytical grade; Fluka
12. Cobalt naphthenate: Analytical grade; Fluka
13. Oleic acid was obtained commercially.
15. Nitrogen gas; Siam Industial Gas
16. Iodine: Analytical grade; Fluka
17. Iodine teichloride: Analytical grade; Fluka
18. Potassium iodide: Analytical grade; Merck
19. Starch: Reagent grade; Merck
20. Sodium thiosulfate: Analytical grade; Fluka

21.Potassium dichromate: Analytical grade; Merck

22.Talcum clay (Utaradit Province); Cernic international Co.,Ltd.

23.China Clay (Ranong Province); Cernic international Co.,Ltd.

24.Ball clay (Suratthani Province); Cernic international Co.,Ltd.

3.2 Apparatus and Instruments

1. Fourier-Transform NMR Spectrometer: Model AC-F 200 (200 MHz); Bruker Spectrospin
2. Fourier-Transform Infrared Spectrophotometer (FT-IR): Model Impact 410; Nicolet
3. Matrix-Assisted Laser Desorption Ionization Mass spectrometer (MALDI-MS); Biflex, Bruker
4. Hotplate magnetic stirrer; Jenway 1100
5. Rotary evaporator; Büchi, R-114
6. Apparatus for determining the Iodine value (I.V.) of the oil

   6.1 Burette (50 ml).

   6.2 Graduate pipette (1, 5 and 10 ml).

   6.3 Glass stopper volumetric flask

   6.4 Stand and clamp for supporting burette

3.3 Experimental

3.3.1 The acid activation of clay [11]

Fifty grams of clay was refluxed with 250 ml of 4 N H_2SO_4 in a round bottom flask at 90 ^{0}C for 2 hours. The slurry was cooled in air and filtered through a sintered glass crucible. The filter cake was repeatedly washed with distilled water until the filtrate was neutral to litmus paper and drier at 110 ^{0}C, 3 hr.

3.3.2 Determination of clay properties [35]

3.3.2.1 Acidity

Acidity of clays was determined by volumetric titration. In this method, 0.5 g of the clay, previously dried at 120 ^{0}C for 6 hours, was taken into a conical flask to which 15 ml of 0.1N NaOH was added. After stirring the flask for 10 minutes, excess NaOH was titrated with 0.1N H_2SO_4 . Acidity was determined as milliequivalents of NaOH used per 100g of clay.

$$\text{Acidity of clay (meq/100 g clay)} = \frac{(V1-V2) \times [H_2SO_4] \times 100}{\text{amount of clay}}$$

Where: V1 is the volume of NaOH, V2 is the volume of H_2SO_4 , and $[H_2SO_4]$ is the H_2SO_4 concentration.

3.3.3 Determination of iodine value

The iodine value is defined by the amount of halogen (calculated by the number of grams of iodine) absorbed by 100 g of the sample. The iodine values of the sample were determined following the Japanese Industrial Standard JIS K 0070-1966 (see Appendix B).

About 3 g of the sample was weighed accurately into 250 ml iodine flask and 10 ml of Wijs's solution was added and tightly stopper with a glass stopper wet with potassium iodine solution (5%) in order to prevent volatilization of iodine and gently swirl the flask. The flask was kept in a dark place at room temperature for 30 minutes and the flask was swirled occasionally.

Aliquot of 50 to 70 ml of potassium iodine solution (5%) was added, swirl the flask and titrate with N/10 thiosulfate solution until the solution turns pale yellow. Then, one ml of starch solution was added and the titration was continued, with swirling, until the blue color of iodine-starch disappears. The blank titration was carried out in the same manner.

Calculation of the iodine value, I.V., by the following formula:

$$\text{I.V.} = \frac{(B-A) \times f \times 1.269}{S}$$

Where : **A** is the volume of N/10 solution consumed in actual titration (ml), **B** is the volume of N/10 sodium thiosulfate solution consumed in blank titration (ml), **f** is the factor of N/10 sodium thiosulfate solution and **S** is the weight of sample (g).

3.3.4 Dimerization of methyl oleate

3.3.4.1 Synthesis of Methyl Oleate

Oleic acid (100 g) was added to a 500 ml two-neck round bottom flask, equipped with thermometer and reflux condenser. Methanol (250 g) was added along with 96% sulfuric acid (7 g) and the mixture was refluxed at 80 ^{0}C for 6 hours. After the reaction was completed, the mixture was allowed to separate. The organic layer was extracted with water and dichloromethane. After aqueous layer was separated, the organic layer was neutralized with 10% sodium hydrogen carbonate and washed again with water. The solution was dried over anhydrous sodium sulfate. The organic solvent was removed on a rotary evaporator at 60 ^{0}C to give 98.50 g of methyl oleate (98.50 %yield) as a colorless liquid.

3.3.4.2 Dimerization of methyl oleate using clay as a catalyst

Methyl oleate (1 g) and clay (10-35 %wt.) was added into a 25 ml two-necked round bottom flask, equipped with thermometer and the mixture was heated at temperature 230- 270 ^{0}C under nitrogen and stirred for a period of 1-6 hours. At the end the mixture was cooled to 100-140 ^{0}C. Then, clay was removed by filtration. This product was purified by SiO_2 column chromatography eluted with the mixture of hexane-ethyl acetate (75:25).

3.3.4.3 Dimerization of methyl oleate using cobalt naphthenate as a catalyst

Methyl oleate (1 g) and cobalt naphthenate (0.03-0.09 %wt.) was added into a 25 ml two-necked round bottom flask. A vigorous stream of air was passed through the solution at 70 ^{0}C and stirred for a period of 12-168 hours. This product was purified by SiO_2 column chromatography eluted with the mixture of hexane-ethyl acetate (75:25).

3.3.4.4 Dimerization of methyl oleate using *tert*-butylhydroperoxide and cobalt naphthenate as a catalyst

Methyl oleate (1 g), *tert*-butylhydroperoxide (0.5-2.0 %wt.) and cobalt naphthenate (0.05-0.09 %wt.) were added into a 25 ml two-necked round bottom flask. A vigorous stream of air was passed through the solution at room temperature and stirred for a period of 24-120 hours. This product was purified by SiO_2 column chromatography eluted with the mixture of hexane-ethyl acetate (75:25).

3.3.4.5 Dimerization of methyl oleate using *tert*-butylhydroperoxide, cobalt naphthenate and clay as a catalyst

Methyl oleate (1 g), *tert*-butylhydroperoxide (1.5 %wt.), cobalt naphthenate (0.05 %wt.) and clay (10-35 %wt.) were added into a 25 ml two-necked round bottom flask. A vigorous stream of air was passed through the solution at 60 ^{0}C and stirred for a period of 24 hours. The product was purified as above.

3.4 Characterization of Dimers

The synthetic of dimer were characterized by spectroscopic techniques including :

1. Fourier-Transform Infrared Spectroscopy
2. Fourier-Transform NMR Spectroscopy
3. Matrix-Assisted Laser Desorption Ionization- Mass spectroscopy

CHAPTER IV

RESULTS AND DISCUSSION

4.1 Determination of clay properties [35]

The difference in properties of acid-activated and non acid-activated clays in terms of structure and acidity of the clay samples were determined.

4.1.1 Acidity characterization

Figure 4.1 shows the total acidity of clay, determined by sodium hydroxide titrations and expressed in meq of NaOH used per 100 g of clay. Talcum after acid activation exhibited the maximum acidity (78.53 meq/100 g) followed by china and ball clay, respectively.

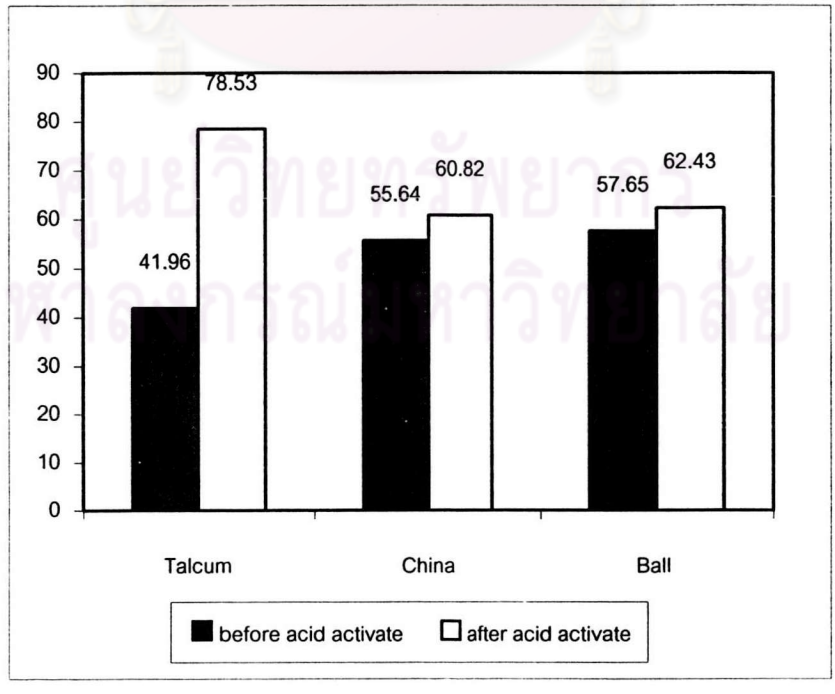

Figure 4.1 Acidity values of clays before and after acid activation

4.1.2 Study of clay structure

The surfaces of clay samples were observed using ScanninElectron Microscope (SEM), and the values of 48.27-56.23, 26.20-30.53 and 22.49-26.20 μm. were found for talcum, china and ball clay, respectively. The surface of talcum was found to have more porosity than the others. Thus, they should have more acid sites than the others.

IR spectroscopy is very sensitive to the structure changes, which occurs in the clay upon acid treatment. Figures B1-B2 show IR spectra of acid activated clay samples, and Table 4.1 summarizes the main vibrations observed. Figures 4.2 indicates that the intensity of the band between 3800 and 3300 cm^{-1} decreased in acid activated talcum.

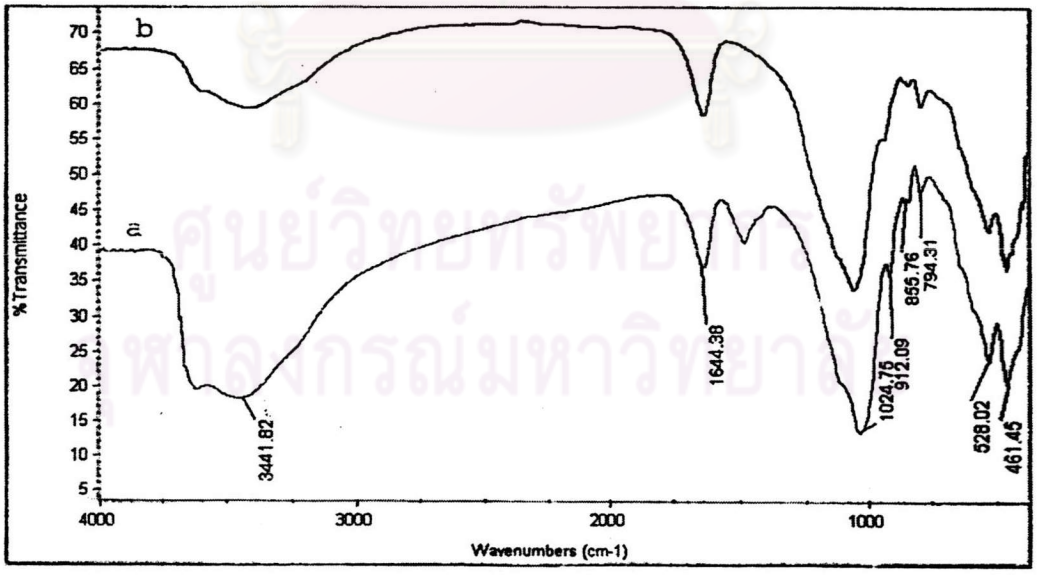

Figure 4.2 FTIR spectra of talcum (a) non-acid activated ; (b) acid activated with H_2SO_4

Moreover, the Si-O band, shift from 1024 to 1045 cm^{-1}, indicated that the acid treatment had attacked the present clay structure. The band nearby 915 cm^{-1} corresponding to the AlAlOH bending deformation decreased and became very weak for acid treated talcum, suggesting a significant depopulation of the octahedral sheet by acid treatment.

Table 4.1 Characteristic FTIR absorption bands for acid activated clays.

Wavenumber (cm^{-1}) of Talcum		Band assignment
Parent	Acid[a]	
3441	3441 [b]	OH stretching
1644	1644 [b]	Hydration,HOH deformation
1024	1045	SiO stretching
912	912 [b]	OH deformation

a = acid activated clay
b = intensity decreased

On the other hand, Figures B1-B2 show no difference of IR spectra between china and ball clays. Therefore, the acid activation of these clays did not change the structure by acid treatment.

4.2 Dimerization of methyl oleate

4.2.1 Synthesis of methyl oleate

Methyl oleate could be prepared from esterification of oleic acid using concentrated sulfuric acid as a catalyst, the product obtained was colorless liquid in 98.50 percent yield (Iodine Value = 81.27).

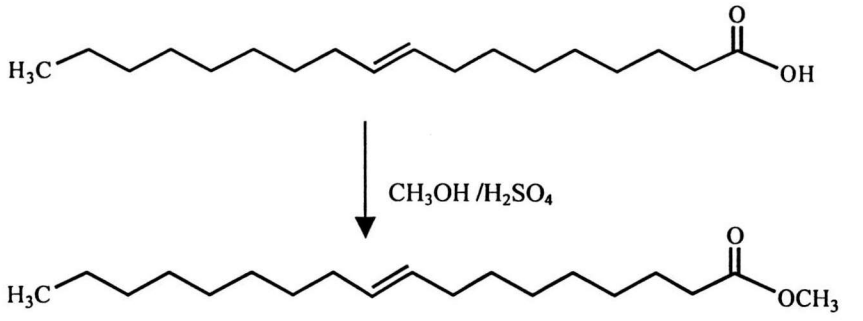

methyl oleate (m/z 296)

Figure 4.3 Synthesis of methyl oleate

4.2.2 Characteristics of methyl oleate

The IR spectra of oleic acid and methyl oleate are shown in Figures B6 and B9, respectively. The important absorption bands of oleic acid and methyl oleate are listed in Table 4.2.

Table 4.2 The IR absorption bands assignment of oleic acid and methyl oleate.

Wavenumber (cm^{-1})		Assignments
Oleic acid	Methyl oleate	
3300	-	O-H Stretching
3001	3002	=C-H Stretching
2847	2851	C-H Stretching, Aliphatic
1705	1731	C=O Stretching
1454	1462	C-H Bending, Aliphatic
1291	1168	C-O Stretching

The ^{1}H-NMR and ^{13}C-NMR spectra of oleic acid and methyl oleate are shown in Figures B7, B8, B10 and B11, respectively. Some signals of oleic acid and methyl oleate are shown in Table 4.3

Table 4.3 The assignments of ^{1}H-NMR and ^{13}C-NMR spectra of oleic acid and methyl oleate.

Position of proton	Chemical shift (δ, ppm)			
	Oleic acid		Methyl oleate	
	^{1}H	^{13}C	^{1}H	^{13}C
a	0.91	14.07	0.88	14.03
b	1.45	22.57	1.42	22.55
c	1.58	24.64	1.55	24.85
d	1.45	27.17	1.45	27.14
e	1.29	29.35	1.26	29.31
f	1.29	31.51	1.26	31.65
g	2.01	34.24	1.96	34.12
h	2.31	34.24	2.28	34.12
i	5.38	127.92,129.95	5.32	128.01,129.51
j	-	179.46	-	-
k	10.34	-	-	-
l	-	-	-	174.20
m	-	-	3.65	51.28

The molecular weight of methyl oleate (m/z 296) is shown in the EIMS spectrum (Figure 4.4).

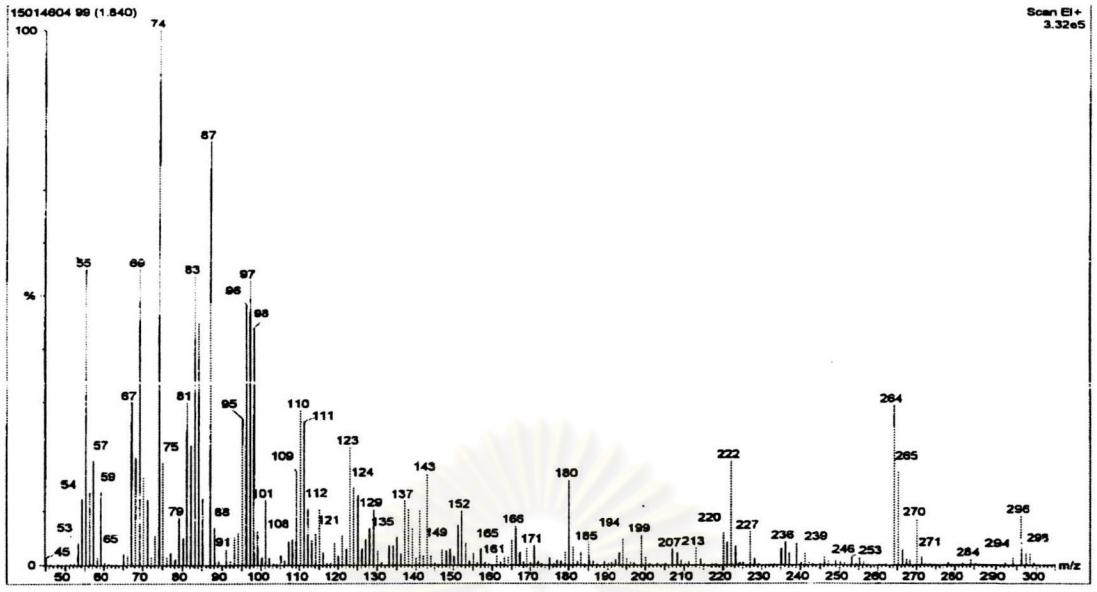

Figure 4.4 EIMS spectrum of methyl oleate

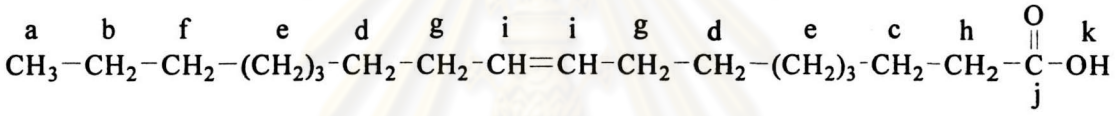

Oleic acid

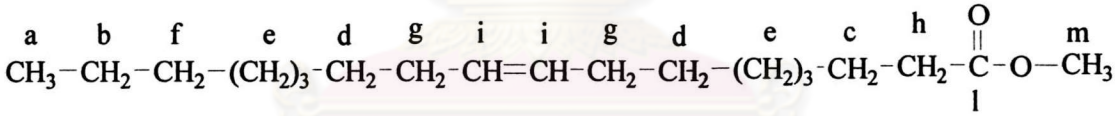

Methyl Oleate

4.2.3 Dimerization of methyl oleate using clays as catalysts

4.2.3.1 Effect of the content of clay

In this section, the content of clay on dimerization of methyl oleate was varied at 10, 15, 20, 25, 30 and 35 %wt at 250 ^{0}C, 4 hr. The result indicated that increasing % wt of clay led to the increase in percent yield of dimer until the content of clay was around 30 to 35 %wt. The yield of dimer was slightly declined

(Figure 4.5). Therefore, 25%wt of clay was selected as the optimum content of clay used in the dimerization reaction.

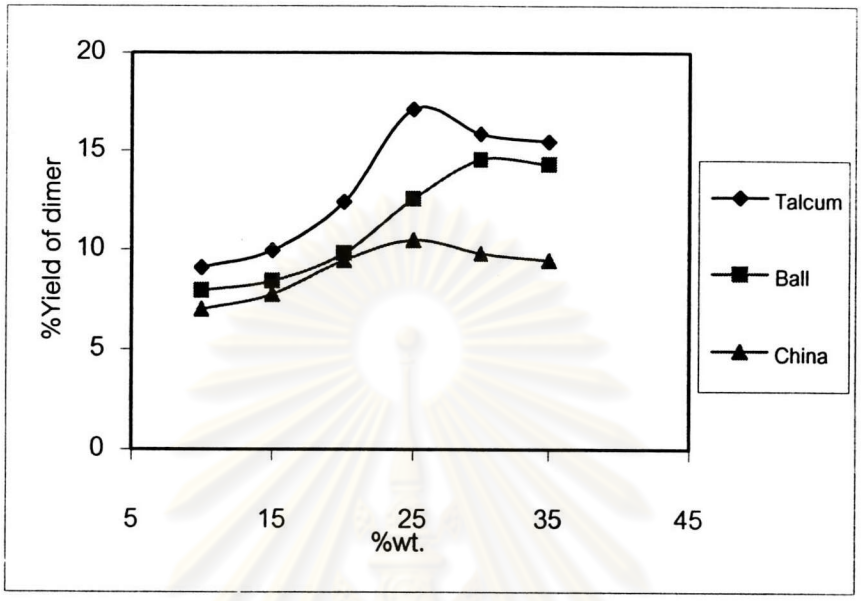

Figure 4.5 Effect of clay content on %yield of dimer at 250 ^{0}C, 4 hr.

4.2.3.2 Effect of the reaction temperature

In this section, the effect of reaction temperature on dimerization of methyl oleate was varied at 230, 250 and 270 ^{0}C at 4 hr. using 25 %wt of clay. The result indicated that increasing the reaction temperature from 230 to 250 ^{0}C also increased the dimer product. However, the use of high reaction temperature (270 ^{0}C) led to the decrease of dimer product (Figure 4.6). Thus, the temperature at 250 ^{0}C was selected for dimerization reaction.

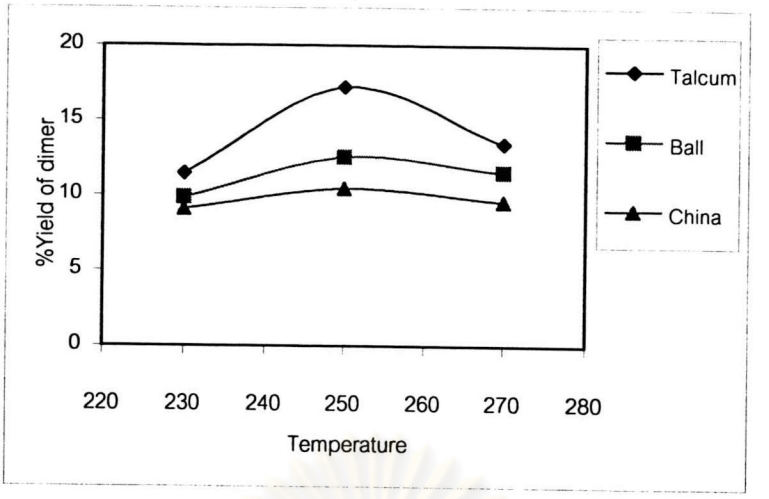

Figure 4.6 Effect of temperature on %yield of dimer at 4 hr. and 25%wt clay.

4.2.3.3 Effect of the reaction time

In this section, the effect of reaction time on dimerization of methyl oleate was varied at 1, 2, 3, 4, 5 and 6 hr. at 250 ^{0}C, 25 %wt of clay. The result indicated that maximum yield of dimer were reached within 4 hr., (Figure 4.7). So that, the reaction time was selected at 4 hrs.

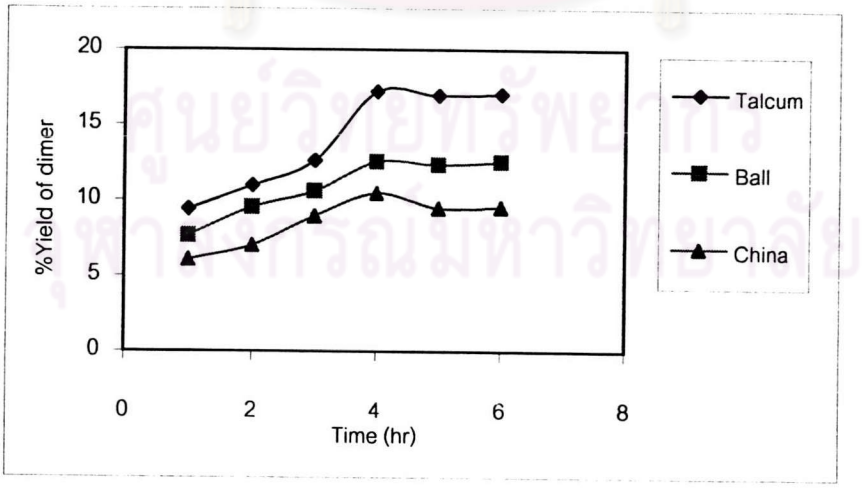

Figure 4.7 Effect of reaction time on %yield of dimer at 250 ^{0}C and 25%wt clay.

The product (Iodine Value = 51.93) obtained from the dimerization reaction was yellow viscous liquid. Clays could be ranked according to the % dimerization as talcum (17.20%) > ball (12.55%) > china (10.47%).

4.2.3.4 Characteristics of dimer obtained from methyl oleate using clay as a catalyst

The IR spectra of methyl oleate and dimer are shown in Figures B9 and B12, respectively. The important absorption bands of methyl oleate and dimer are listed in Table 4.4.

Table 4.4 The IR absorption bands assignment of methyl oleate and dimer

Wavenumber (cm^{-1})		Assignments
Methyl oleate	Dimer	
2851	2861	C-H Stretching, Aliphatic
1731	1711	C=O Stretching
1462	1472	C-H Bending, Aliphatic
1168	1158	C-O Stretching

The ^{1}H-NMR and ^{13}C-NMR spectra of methyl oleate and dimer are shown in Figures B10, B11, B13 and B14, respectively. Some signals of methyl oleate and dimer are shown in Table 4.5.

Table 4.5 The assignments of ^{1}H-NMR and ^{13}C-NMR spectra of methyl oleate and dimer using clay as a catalyst.

Position of Proton	Chemical Shift (δ, ppm)			
	Methyl oleate		Dimer	
	^{1}H	^{13}C	^{1}H	^{13}C
a	0.88	14.03	0.85	13.98
b	1.45	22.55	1.42	22.50
c	1.55	24.85	1.53	24.81
d	1.45	27.14	1.42	27.09
e	1.26	29.31	1.22	29.27
f	1.26	31.65	1.22	31.59
g	1.96	34.12	1.94	34.08
h	2.28	34.12	2.23	34.08
i	5.32	128.01,129.51	5.28	129.01,129.62
j	-	174.20	-	174.41
k	3.65	51.28	3.59	51.02
l	-	-	1.48	38.92
m	-	-	2.15	42.03

The molecular weight of dimer obtained from methyl oleate was investigated using Matrix-assisted laser desorption/ionization mass spectrometry (MALDI-MS) with CCA as the matrix. The results was shown in figure 4.8.

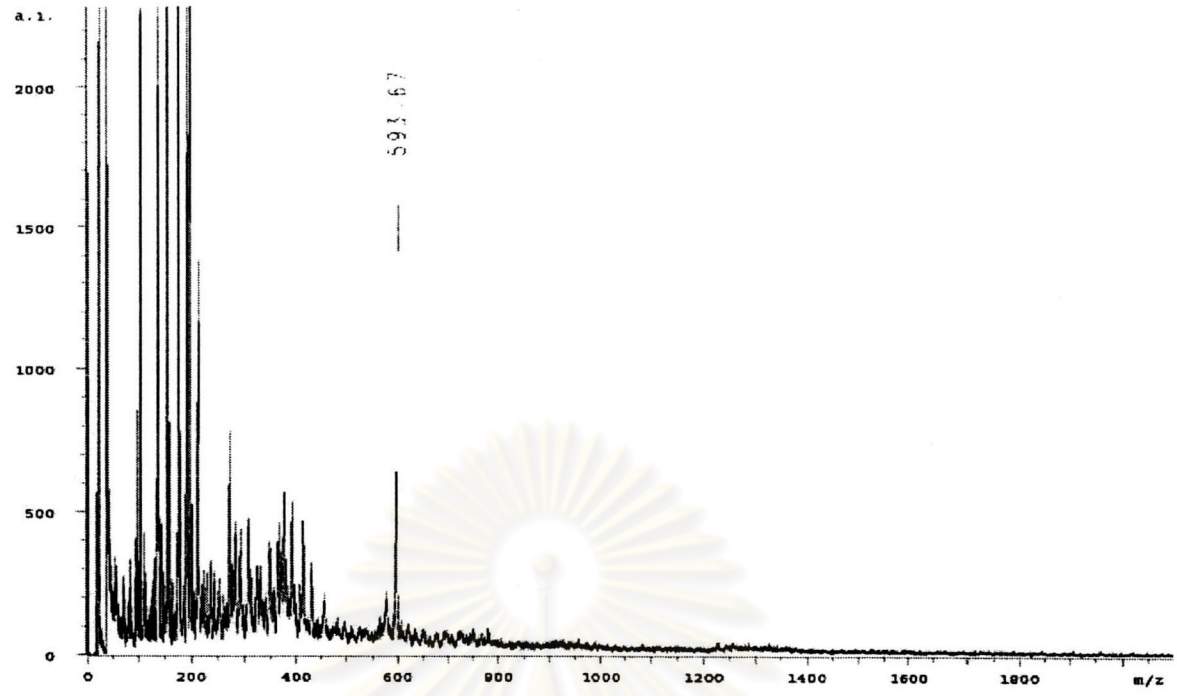

Figure 4.8 MALDI spectrum of dimer obtained from methyl oleate using clay as a catalyst.

The chemical equation of the reaction was represented as in Figure 4.9.

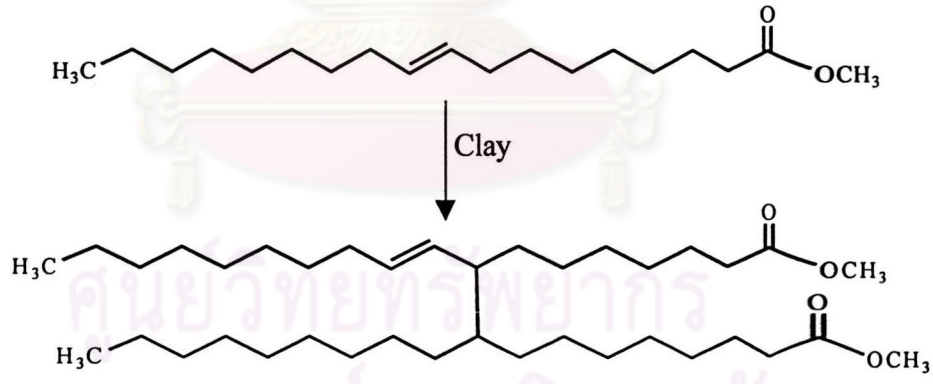

$[C_{38}H_{72}O_4 + H^+]$; MW.= 593

Figure 4.9 The proposed structure of dimer obtained from methyl oleate using clay as a catalyst.

4.2.3.5 Mechanism of dimerization methyl oleate (carbocation mechanism)

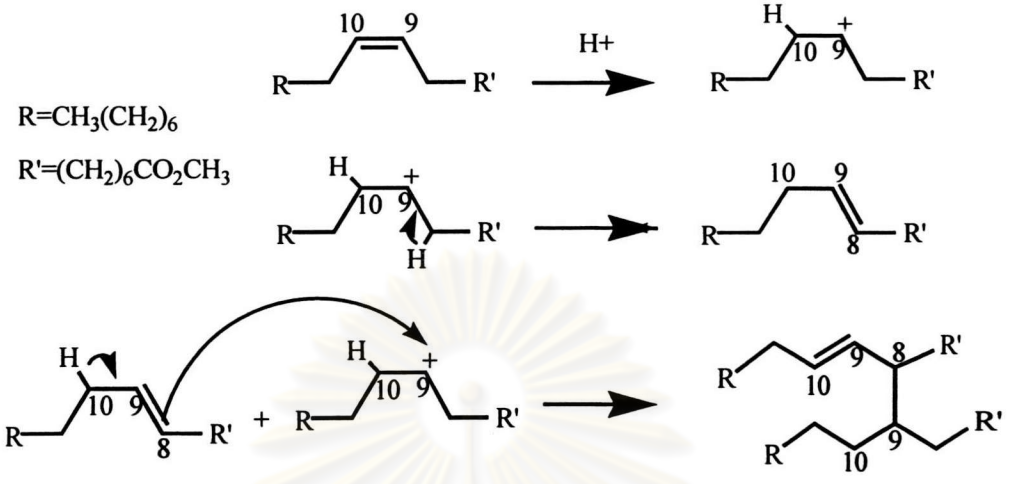

From the results of table 4.5, it could be concluded that the product was dimer and its proposed structure is shown below:

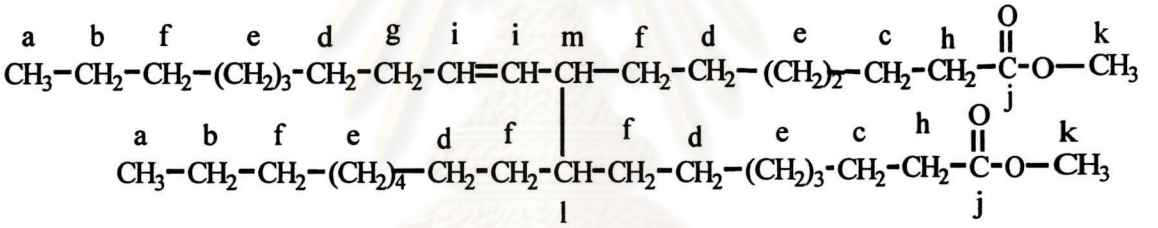

4.2.4 Dimerization of methyl oleate using cobalt naphthenate as a catalyst at room temperature

4.2.4.1 Effect of the content of cobalt naphthenate

In this section, the content of cobalt naphthenate on dimerization of methyl oleate was varied from 0.03, 0.05, 0.07 to 0.09 %wt at room temperature, (Figure 4.10). The result indicated that at reaction time of 72 hr., increasing the reaction content of cobalt naphthenate from 0.03 to 0.09%wt also increased the dimer product. However, at the long reaction time, the increasing reaction content of cobalt

naphthenate from 0.05 to 0.09%wt was not significant. Therefore, 0.05 %wt of cobalt naphthenate was selected as the optimum content to used in the dimerization reaction.

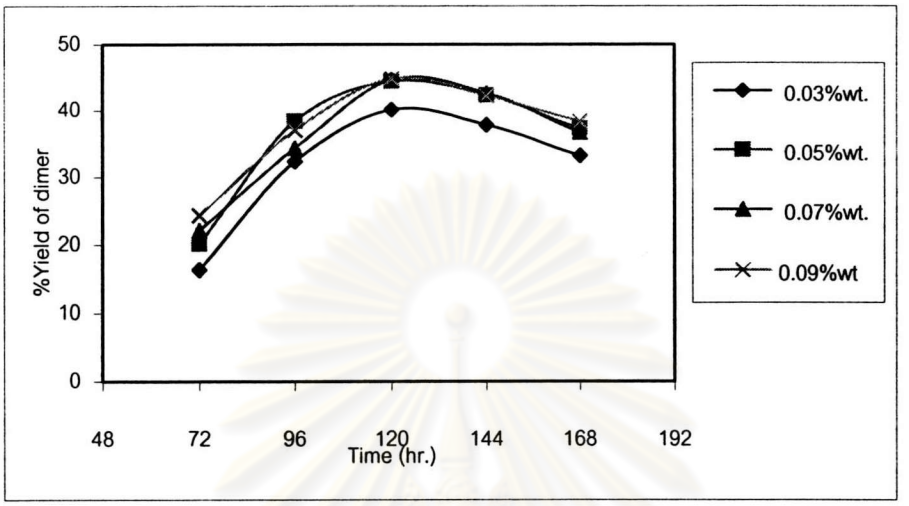

Figure 4.10 Effect of cobalt naphthenate content on %yield of dimer at room temperature.

4.2.4.2 Effect of the reaction time

In this section, the effect of reaction time on dimerization of methyl oleate was varied from 72, 96, 120, 144 to 168 hr. at room temperature, and 0.05 %wt of cobalt naphthenate (Figure 4.10). The result indicated that maximum yield of dimer was reached within 120 hr. After that, increasing the reaction time from 120 to 168 hr., decreased the dimer product. Thus, the reaction time at 120 hr was selected for dimerization.

Under the optimum condition on the dimerization of methyl oleate with 0.05%wt cobalt naphthenate and 120 hr at room temperature. The product was obtained as yellow viscous liquid in 44.45 percent yield (Iodine Value = 95.36).

4.2.4.3 Characteristics of dimer obtained from methyl oleate using cobalt naphthenate as a catalyst at room temperature

The IR spectra of methyl oleate and dimer are shown in Figures B9 and B16, respectively. The important absorption bands of methyl oleate and dimer are listed in Table 4.6.

Table 4.6 The IR absorption bands assignment of methyl oleate and dimer

Wavenumber (cm^{-1})		Assignments
Methyl oleate	Dimer	
-	3472	O-H Stretching
2851	2863	C-H Stretching, Aliphatic
1731	1725	C=O Stretching
1462	1468	C-H Bending, Aliphatic
1168	1162	C-O Stretching

The ^{1}H-NMR and ^{13}C-NMR spectra of methyl oleate and dimer are shown in Figures B10, B11, B17 and B18, respectively. Some signals of methyl oleate and dimer are shown in Table 4.7.

Table 4.7 The assignments of ^{1}H-NMR and ^{13}C-NMR spectra of methyl oleate and dimer using cobalt naphthenate catalyst at room temperature.

Position of Proton	Chemical Shift (δ, ppm)			
	Methyl oleate		Dimer	
	^{1}H	^{13}C	^{1}H	^{13}C
a	0.88	14.03	0.82	13.89
b	1.45	22.55	1.43	22.46
c	1.55	24.85	1.50	24.77
d	1.45	27.14	1.43	27.04
e	1.26	29.31	1.23	29.26
f	1.26	31.65	1.23	31.54
g	1.96	34.12	1.92	34.05
h	2.28	34.12	2.24	34.05
i	5.32	128.01,129.51	5.24	128.33,129.48
j	-	174.20	-	174.05
k	3.65	51.28	3.57	50.69
l	-	-	4.21	82.46
m	-	-	3.53	74.62
n	-	-	2.21	42.15

The molecular weight of dimer obtained from methyl oleate using cobalt naphthenate as a catalyst at room temperature was investigated using Matrix-assisted laser desorption/ionization mass spectrometry (MALDI-MS) with CCA as the matrix. The result was shown in figure 4.11.

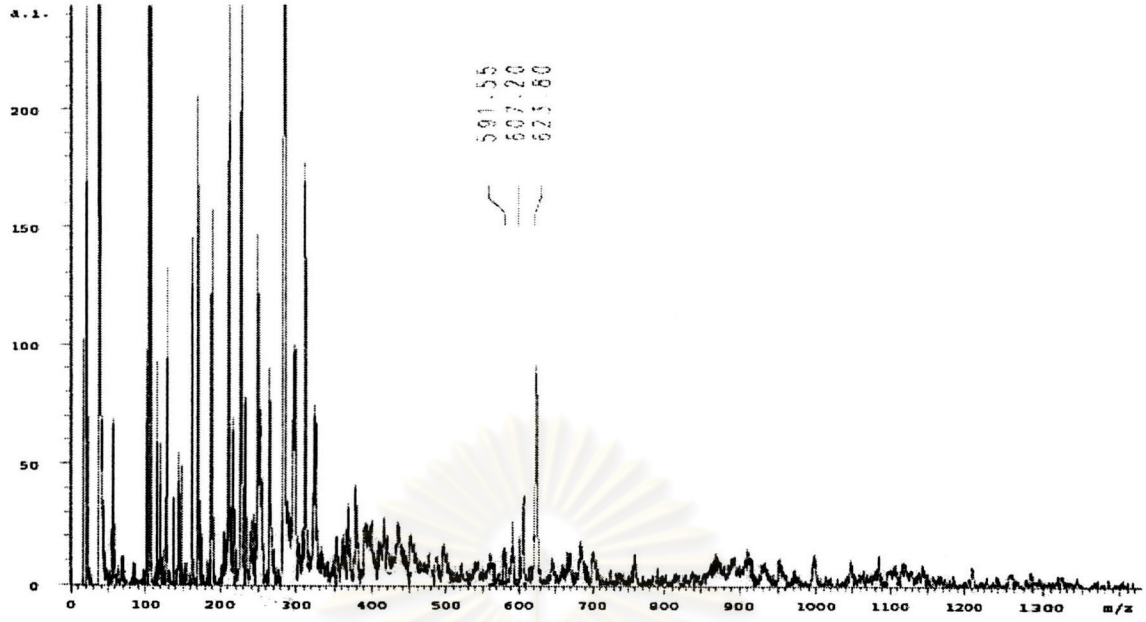

Figure 4.11 MALDI spectra of dimer obtained from methyl oleate using cobalt naphthenate as a catalyst at room temperature.

The dimerization was represented as an example in Figure 4.12.

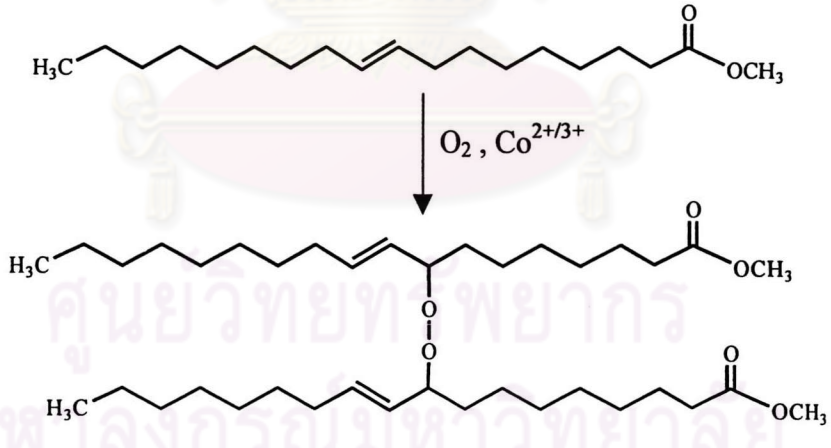

$[C_{38}H_{70}O_6 + H^+]$; MW.= 623

+

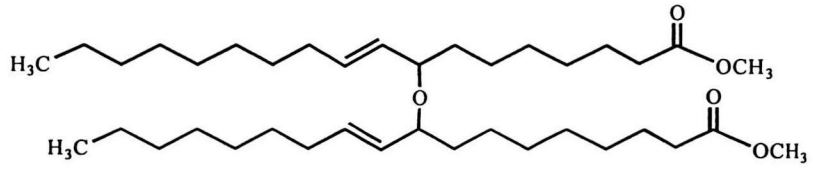

$[C_{38}H_{70}O_5 + H^+]$; MW.= 607

+

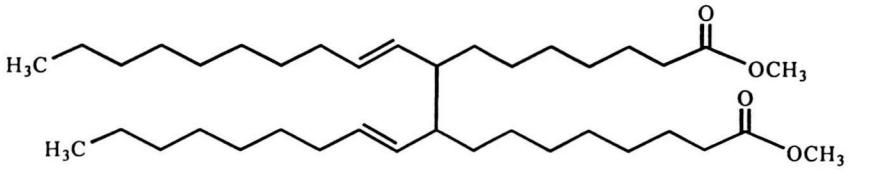

$[C_{38}H_{70}O_4 + H^+]$; MW.= 591

Figure 4.12 The proposed structure of dimer obtained from methyl oleate using cobalt naphthenate as a catalyst at room temperature.

4.2.4.4 Mechanism of dimerization methyl oleate (free radical mechanism)

Cobalt-catalyzed oxidation of methyl oleate takes place via a radical generate oxygen atom abstraction reaction.

$$Co^{2+} + O_2 \longrightarrow Co^{3+} + {}^{-}O\text{-}O^{\cdot}$$

As $^{-}O\text{-}O^{\cdot}$ is being formed here, this step is an *initiation* reaction.

$$^{-}O\text{-}O^{\cdot} + RH \longrightarrow R^{\cdot} + {}^{-}OOH$$

$R^{\cdot}$ reacts with oxygen in a chain *propagation* reaction :

$$R^{\cdot} + O_2 \longrightarrow ROO^{\cdot}$$

$$ROO^{\cdot} + RH \longrightarrow ROOH + R^{\cdot}$$

ROOH reacts with cobalt in an important *initiation* reaction :

$$Co^{2+} + ROOH \longrightarrow Co^{3+} + RO^{\cdot} + OH^{-}$$

$$Co^{3+} + ROOH \longrightarrow Co^{2+} + ROO^{\cdot} + H^{+}$$

Crosslink formation may now occur by addition to the double bond or by means of combination of radicals :

$$2\,R^{\cdot} \longrightarrow R\text{-}R \text{ (C-C- linked dimer)}$$

$$R^{\cdot} + RO^{\cdot} \longrightarrow ROR \text{ (ether-linked)}$$

$$R^{\cdot} + ROO^{\cdot} \longrightarrow ROOR \text{ (peroxy-linked)}$$

$$2\,RO^{\cdot} \longrightarrow ROOR$$

From the results of table 4.7, it could be concluded that the products were dimers and their structure was as follows:

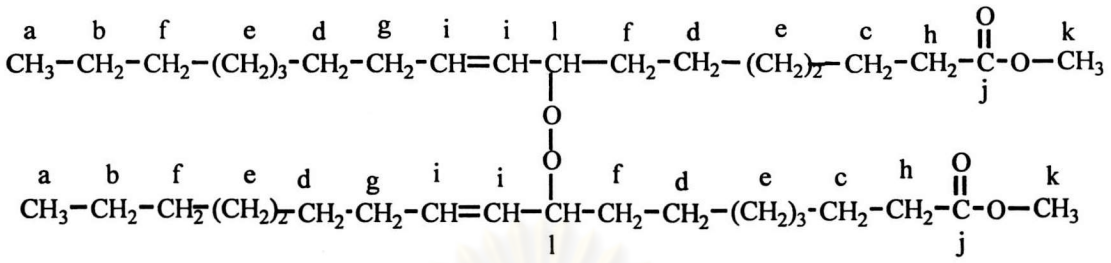

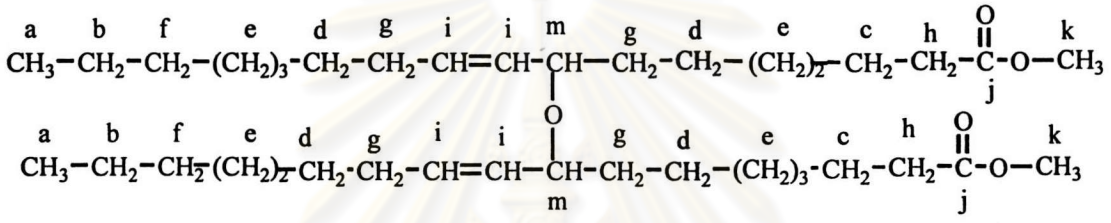

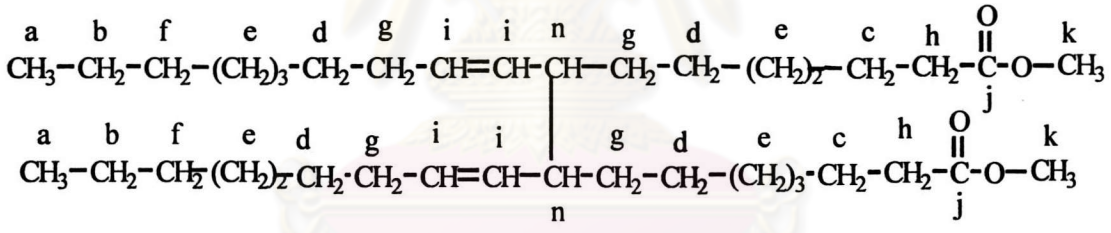

4.2.5 Dimerization of methyl oleate using cobalt naphthenate as a catalyst at 60 ^{0}C

4.2.5.1 Effect of cobalt naphthenate content

In this section, the content of cobalt naphthenate on dimerization of methyl oleate was varied from 0.03, 0.05, 0.07 to 0.09 %wt at 60 ^{0}C (Figure 4.13). The result indicated that increasing cobalt naphthenate content at the reaction time 12 hr from 0.03 to 0.09 %wt increased the dimer product. However, an increasing to the cobalt

naphthenate content at longer reaction time, did not show any improvement of dimer formation. Therefore, the cobalt naphthenate content was selected at 0.05 %wt.

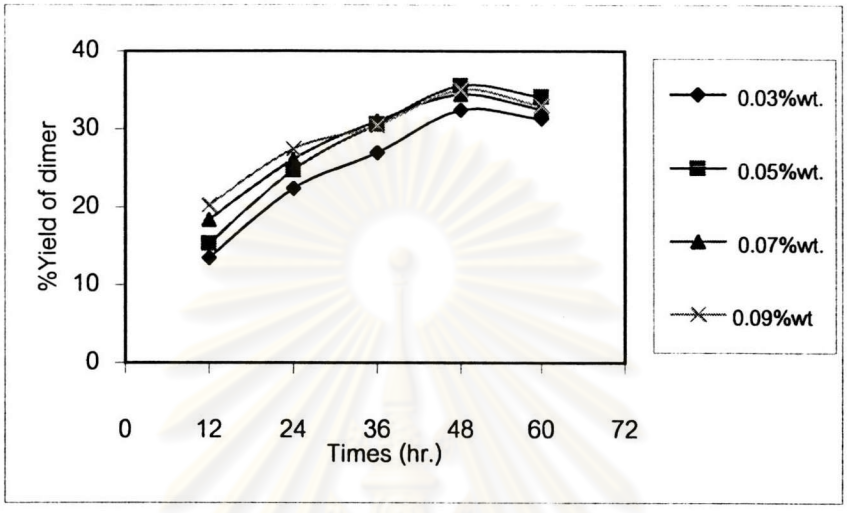

Figure 4.13 Effect of cobalt naphthenate content on %yield of dimer at 60 ^{0}C.

4.2.5.2 Effect of the reaction time

In this section, effect of the reaction time on dimerization of methyl oleate was varied from 12, 24, 36, 48 to 60 hr. at 60 ^{0}C and 0.05 %wt of cobalt naphthenate (Figure 4.13). The result indicated that maximum yield of dimer were reached within 48 hr. After that an increasing the reaction time from 48 to 60 hr. decreased the dimer product. Thus, the reaction time at 48 hr. was selected for dimerization reaction.

Under the optimum condition on dimerization of methyl oleate was 0.05%wt cobalt naphthenate and 48 hr at 60 ^{0}C. The reaction product was yellow viscous liquid with 35.55% yield of dimer (Iodine Value = 96.46).

4.2.5.3 Characteristics of dimer obtained from methyl oleate using cobalt naphthenate as a catalyst at 60 ^{0}C

The IR spectra of methyl oleate and dimer are shown in Figures B9 and B20, respectively. The important absorption bands of methyl oleate and dimer are listed in Table 4.8.

Table 4.8 The IR absorption bands assignment of methyl oleate and dimer.

Wavenumber (cm^{-1})		Assignments
Methyl oleate	Dimer	
2851	2863	C-H Stretching, Aliphatic
1731	1725	C=O Stretching
1462	1468	C-H Bending, Aliphatic
1168	1162	C-O Stretching

The ^{1}H-NMR and ^{13}C-NMR spectra of methyl oleate and dimer are shown in Figures B10, B11, B21 and B22, respectively. Some signals of of methyl oleate and dimer are shown in Table 4.9.

Table 4.9 The assignments of ^{1}H-NMR and ^{13}C-NMR spectra of methyl oleate and dimer using cobalt naphthenate as catalyst at 60 ^{0}C.

Position of Proton	Chemical Shift (δ, ppm)			
	Methyl oleate		Dimer	
	^{1}H	^{13}C	^{1}H	^{13}C
A	0.88	14.03	0.85	13.93
b	1.45	22.55	1.41	22.48
c	1.55	24.85	1.52	24.79
d	1.45	27.14	1.41	27.11
e	1.26	29.31	1.21	29.25
f	1.26	31.65	1.21	31.63
g	1.96	34.12	1.92	34.02
h	2.27	34.12	2.22	34.02
I	5.32	128.01,129.51	5.26	128.21,129.34
j	-	174.20	-	174.12
k	3.65	51.28	3.53	50.88
l	-	-	2.24	42.18
m	-	-	3.51	74.59

The molecular weight of dimer obtained from methyl oleate using cobalt naphthenate as a catalyst at 60 ^{0}C was investigated using Matrix-assisted laser desorption/ionization mass spectrometry (MALDI-MS) with CCA as the matrix. The result was shown in figure 4.14.

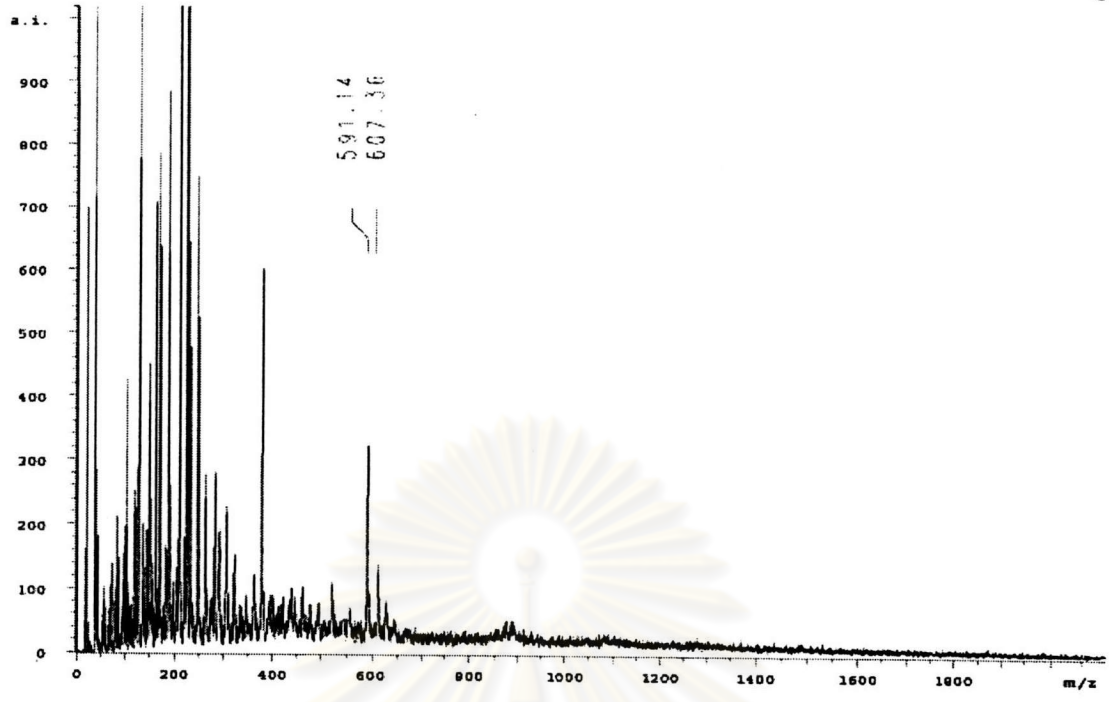

Figure 4.14 MALDI spectrum of dimer obtained from methyl oleate using cobalt naphthenate as a catalyst at 60 ^{0}C.

The chemical equation of the reaction was represented an example in Figure 4.15.

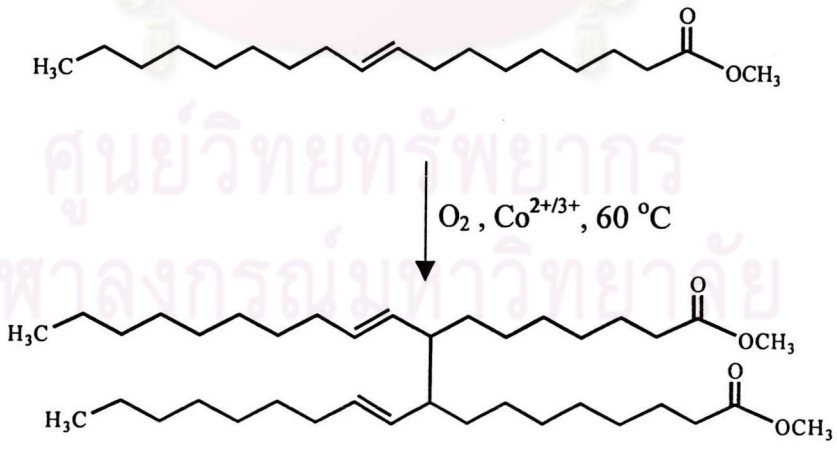

$[C_{38}H_{70}O_4 + H^+]$; MW.= 591

+

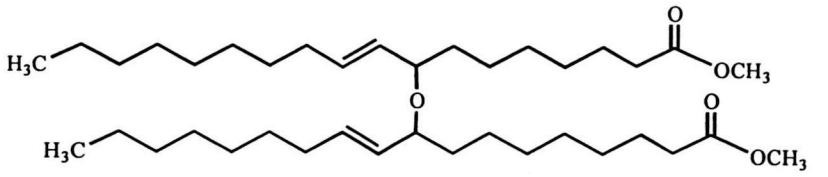

$[C_{38}H_{70}O_5 + H^+]$; MW.= 607

Figure 4.15 The proposed structure of dimer obtained from methyl oleate using cobalt naphthenate as a catalyst at 60 ^{0}C

Mechanism of dimerization of methyl oleate by free radical is shown in 4.2.4.4 From the results of table 4.9, it could be concluded that the product was dimer and its structure was as follow:

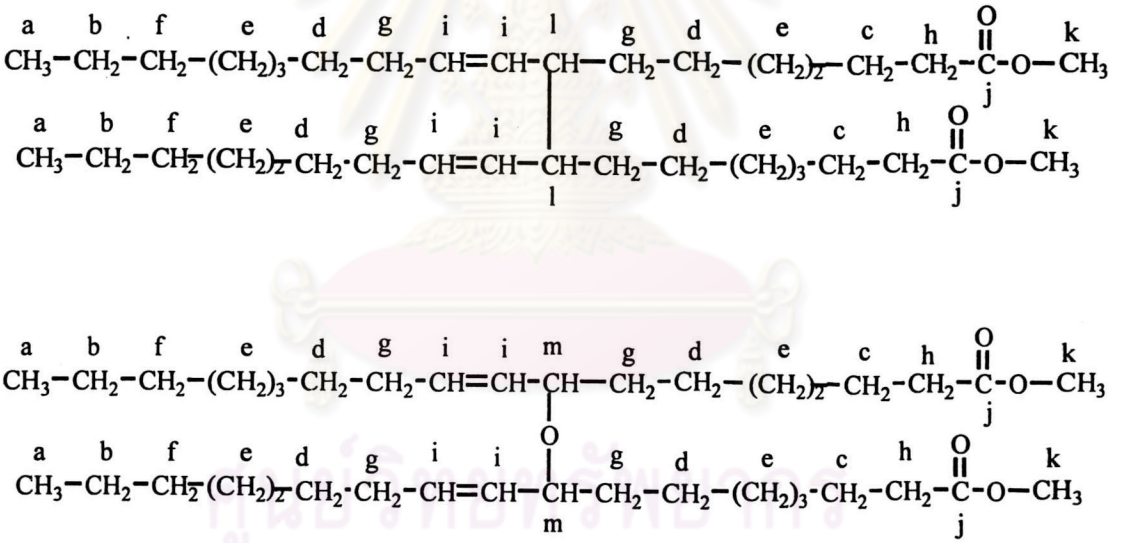

4.2.6 Dimerization of methyl oleate using TBHP and cobalt naphthenate as a catalyst at room temperature

4.2.6.1 Effect of the content of TBHP

In this section, the content of TBHP on dimerization of methyl oleate was varied at 1.0, 1.5 and 2.0 %wt at room temperature and 0.07 %wt of cobalt naphthenate (Figure 4.16). The result indicated that increasing the TBHP content from

1.0 to 1.5 %wt led to the increase in percent yield of dimer. Until, increasing the TBHP content from 1.5 to 2.0 %wt, decreased the dimer product. Thus, 1.5 %wt of TBHP was selected as the optimum content for dimerization reaction.

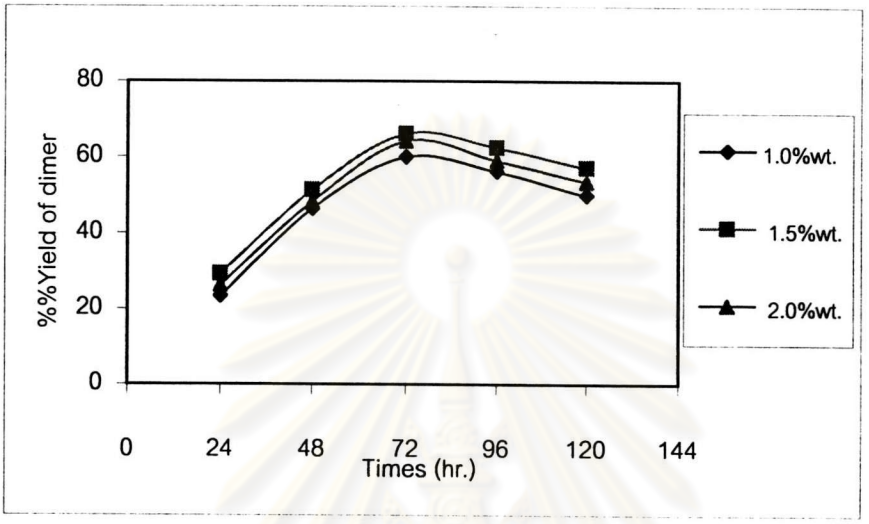

Figure 4.16 Effect of TBHP content on %yield of dimer at room temperature, 0.07%wt cobalt naphthenate.

4.2.6.2 Effect of cobalt naphthenate content.

In this section, the content of cobalt naphthenate on dimerization of methyl oleate was varied from 0.05, 0.07 to 0.09 %wt at room temperature, and 1.5 %wt of TBHP (Figure 4.17). The result indicated that increasing in percent weight of cobalt naphthenate from 0.05 to 0.07 led to the increase in percent yield of dimer. Until, the content of cobalt naphthenate was 0.09 %wt, decreased the dimer product. Thus, 0.07 %wt of cobalt naphthenate was selected as the optimum content in dimerization reaction.

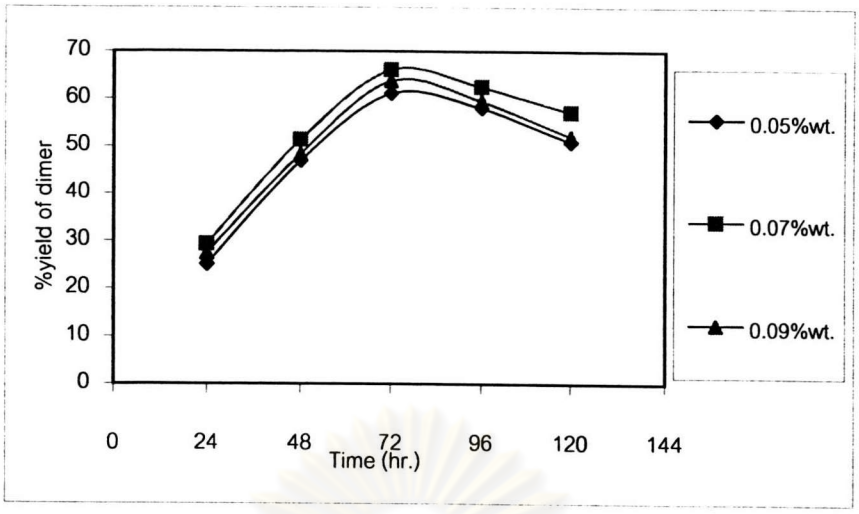

Figure 4.17 Effect of cobalt naphthenate content on %yield of dimer at room temperature, 1.5%wt TBHP.

4.2.6.3 Effect of the reaction time

In this section, the effect of reaction time on dimerization of methyl oleate was varied at 24, 48, 72, 96 and 120 hr. at room temperature, 0.07 %wt of cobalt and 1.5 %wt TBHP as shown in figure 4.16 and 4.17, respectively. The result indicated that increasing the reaction time from 24 to 72 hr. increase the dimer product. However, the longer time of reaction (72 to 120 hr.) led to decrease the dimer product. Thus the reaction time was selected at 72 hr.

Under the optimum condition on dimerization of methyl oleate was 1.5%wt. TBHP, 0.07%wt cobalt naphthenate and 72 hr. at room temperature. The product was yellow viscous liquid at 66.09 % yield of dimer (Iodine Value = 95.67). The chemical equation of the reaction was represented as shown in Figure 4.13. Characteristics of dimer obtained from methyl oleate using TBHP and cobalt naphthenate as a catalyst at room temperature was the same as that obtained from dimerization of methyl oleate using cobalt naphthenate as a catalyst at room temperature (4.2.4).

4.2.7 Dimerization of methyl oleate using TBHP and cobalt naphthenate as a catalyst at 60 ^{0}C

4.2.7.1 Effect of the content of TBHP

In this section, the content of TBHP on dimerization of methyl oleate was varied at 1.0, 1.5 and 2.0 %wt. at 60 ^{0}C and 0.05 %wt of obalt naphthenate (Figure 4.18). The result indicated that increasing the TBHP content led to the increase the diner product. Until, the TBHP content was around 2.0 %wt did not shown any improvement dimer formation. Therefore, 1.5 %wt of TBHP was selected for dimerization reaction.

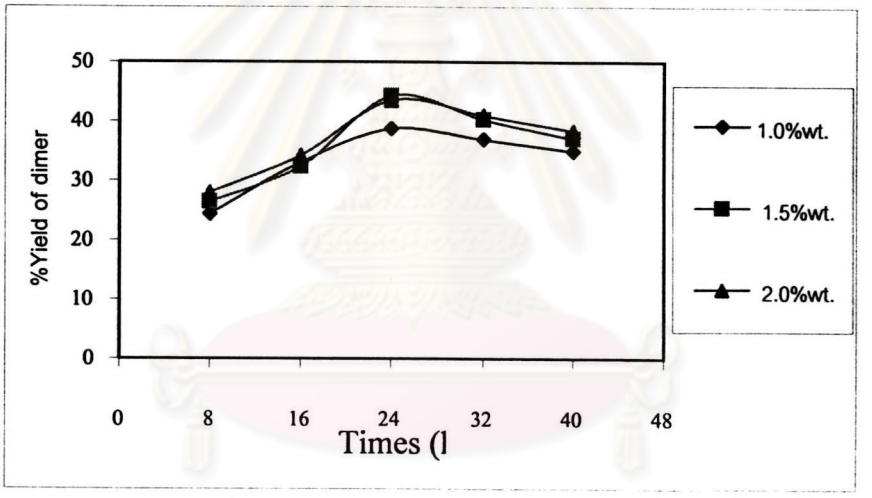

Figure 4.18 Effect of TBHP content on %yield of dimer at 60 ^{0}C and 0.05%wt cobalt naphthenate.

4.2.7.2 Effect of the reaction content of cobalt naphthenate

In this section, the content of cobalt naphthenate on dimerization of methyl oleate was varied at 0.05, 0.07 and 0.09 %wt at 60 ^{0}C and 1.5 %wt of TBHP (Figure 4.19). The result indicated that increasing the cobalt naphthenate content led to decrease the dimer product. Thus, 0.05 %wt of cobalt naphthenate was selected as the optimum content in the dimerization reaction.

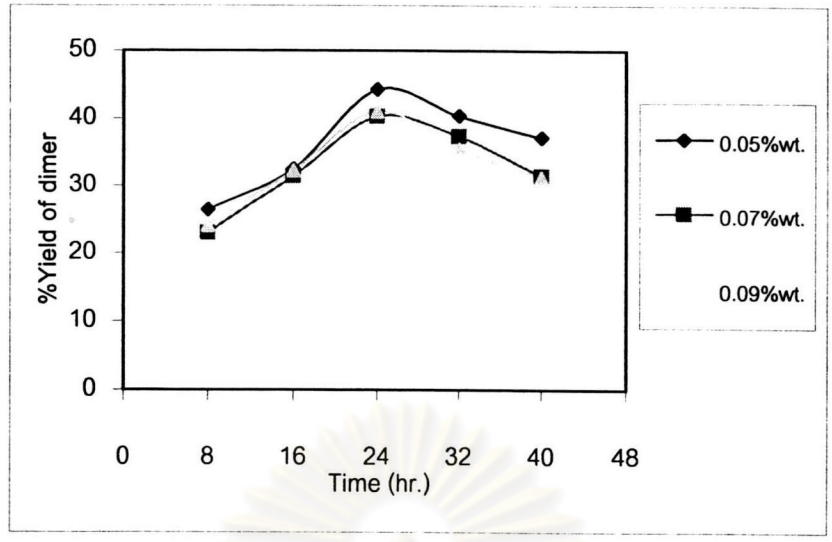

Figure 4.19 Effect of cobalt naphthenate content on %yield of dimer at 60 ^{0}C and 1.5%wt TBHP.

4.2.7.3 Effect of the reaction time

In this section, the effect of reaction time on dimerization of methyl oleate was varied at 8, 16, 24, 32 and 40 hr. at 60 ^{0}C, and 0.05 %wt of cobalt naphthenate and 1.5 %wt TBHP (Figure 4.18 and 4.19). The result indicated that increasing the reaction time led to the increase in percent yield of dimer. Until, the reaction time was around 24 to 40 hr. decrease the dimer product. Therefore, the reaction time was selected at 24 hr.

Under the optimum condition on dimerization of methyl oleate was 1.5%wt TBHP, 0.05%wt cobalt naphthenate and 24 hr. at 60 ^{0}C. The product obtained from dimerization reaction was yellow viscous liquid at 44.28% yield of dimer (Iodine Value = 96.37).

4.2.7.4 Characteristics of dimer obtained from methyl oleate using TBHP and cobalt naphthenate as a catalyst at 60 ^{0}C

The IR spectra of methyl oleate and dimer are shown in Figures B9 and B24, respectively. The important absorption bands of methyl oleate and dimer are listed in Table 4.10.

Table 4.10 The IR absorption bands assignment of methyl oleate and dimer

Wavenumber (cm^{-1})		Assignments
Methyl oleate	Dimer	
2851	2872	C-H Stretching, Aliphatic
1731	1729	C=O Stretching
1462	1463	C-H Bending, Aliphatic
1168	1164	C-O Stretching

The ^{1}H-NMR and ^{13}C-NMR spectra of methyl oleate and dimer are shown in Figures B10, B11, B25 and B26, respectively. Some signals of of methyl oleate and dimer are shown in Table 4.11.

Table 4.11 The assignments of ^{1}H-NMR and ^{13}C-NMR spectra of methyl oleate and dimer using TBHP and cobalt naphthenate as catalyst at 60 ^{0}C.

Position of Proton	Chemical Shift (δ, ppm)			
	Methyl oleate		Dimer	
	^{1}H	^{13}C	^{1}H	^{13}C
a	0.88	14.03	0.83	13.82
b	1.45	22.55	1.42	22.49
c	1.55	24.85	1.53	24.75
d	1.45	27.14	1.42	27.08
e	1.26	29.31	1.22	29.28
f	1.26	31.65	1.22	31.61
g	1.96	34.12	1.93	33.96
h	2.27	34.12	2.24	33.96
I	5.32	128.01,129.51	5.23	128.19,129.43
j	-	174.20	-	174.10
k	3.65	51.28	3.56	50.79
l	-	-	2.22	42.06
m	-	-	3.52	74.62

The molecular weight of dimer obtained from methyl oleate using TBHP and cobalt as a catalyst at 60 ^{0}C was investigated using Matrix-assisted laser desorption/ionization mass spectrometry (MALDI-MS) with CCA as the matrix. The result was shown in figure 4.20.

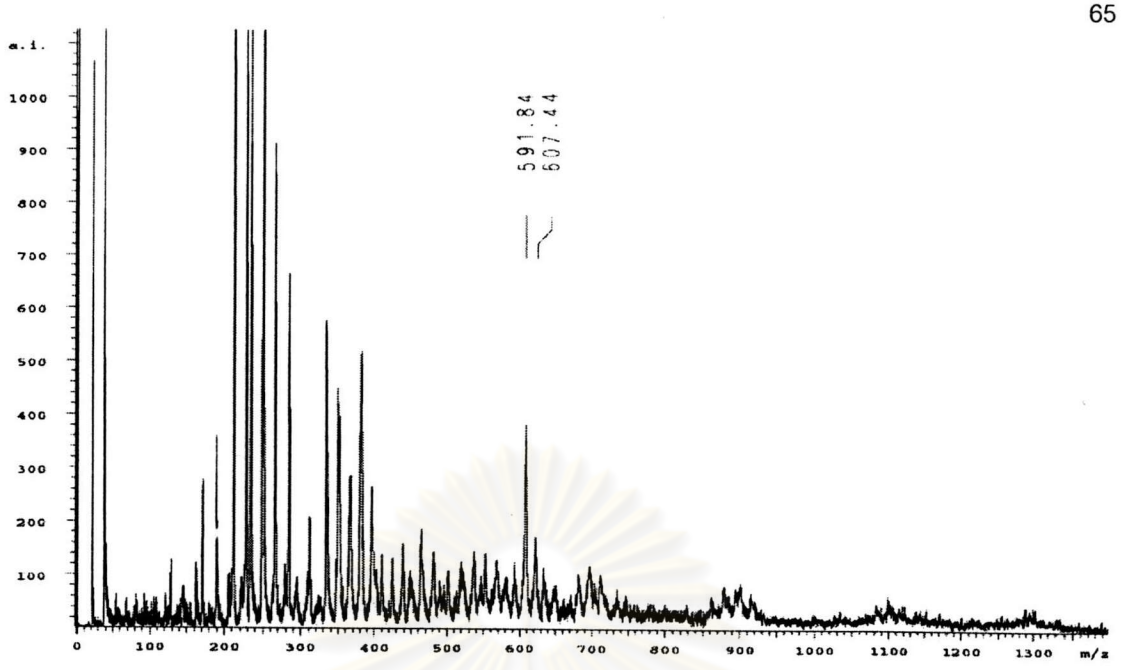

Figure 4.20 MALDI spectrum of dimer obtained from methyl oleate using TBHP and cobalt naphthenate as a catalyst at 60 ^{0}C.

The chemical equation of the reaction was represented as in Figure 4.21

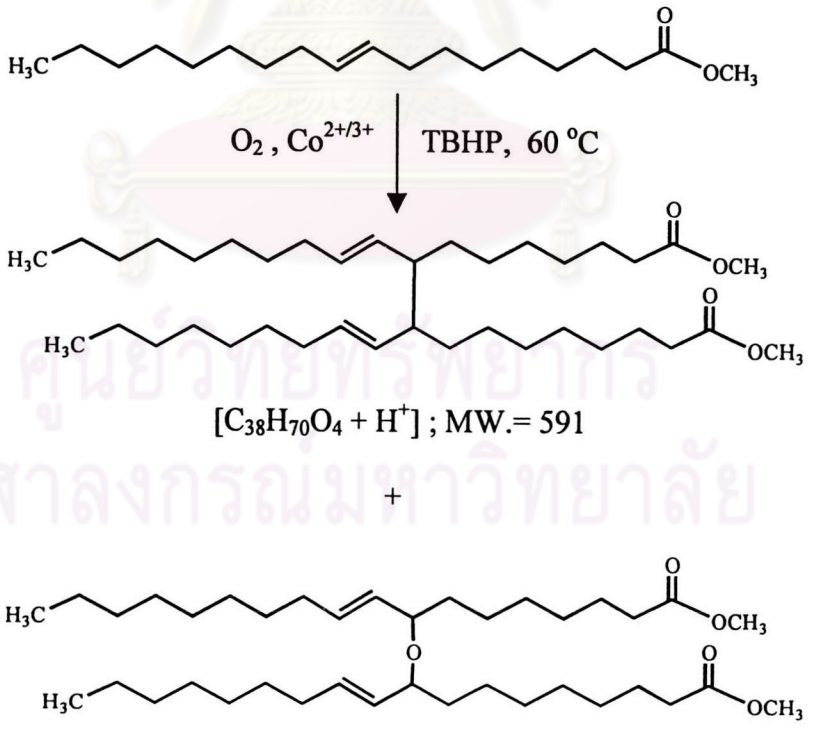

$[C_{38}H_{70}O_4 + H^+]$; MW.= 591

+

$[C_{38}H_{70}O_5 + H^+]$; MW.= 607

Figure 4.21 The proposed structure of dimer obtained from methyl oleate using TBHP and cobalt naphthenate as a catalyst at 60 ^{0}C.

Mechanism of dimerization of methyl oleate by free radical is shown in 4.2.4.4 From the results of table 4.11, it could be concluded that the product was dimer and its structure was as follows:

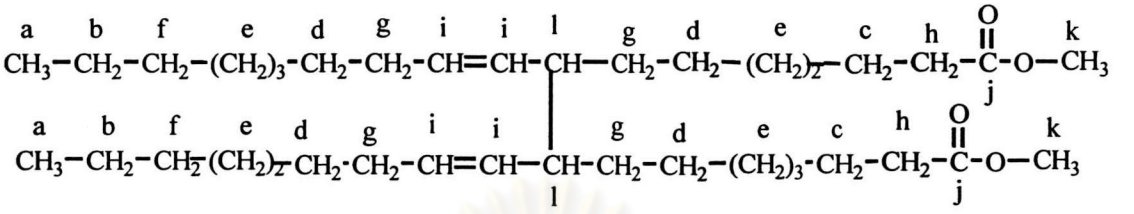

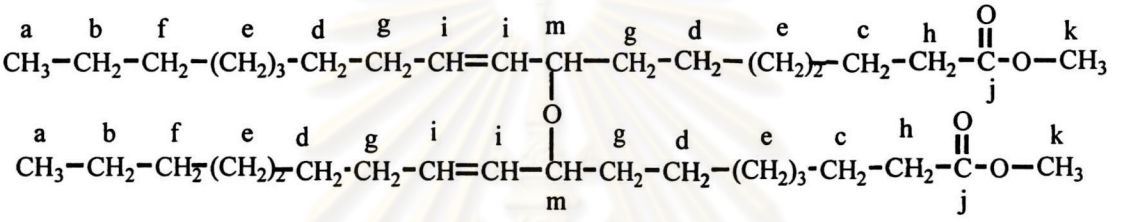

4.2.8 Dimerization of methyl oleate using TBHP, cobalt naphthenate and clay as a catalyst at 60 ^{0}C

4.2.8.1 Effect of the content of clay

In this section, the content of clay the experiments on dimerization of methyl oleate was varied at different content of 10, 15, 20, 25, 30 and 35 %wt at 60 ^{0}C, 24 hr. and 1.5 %wt TBHP and 0.05 %wt of cobalt naphthenate (Figure 4.22). The result indicated that 15 %wt of clay was selected as the optimum content of clay used in the dimerization reaction.

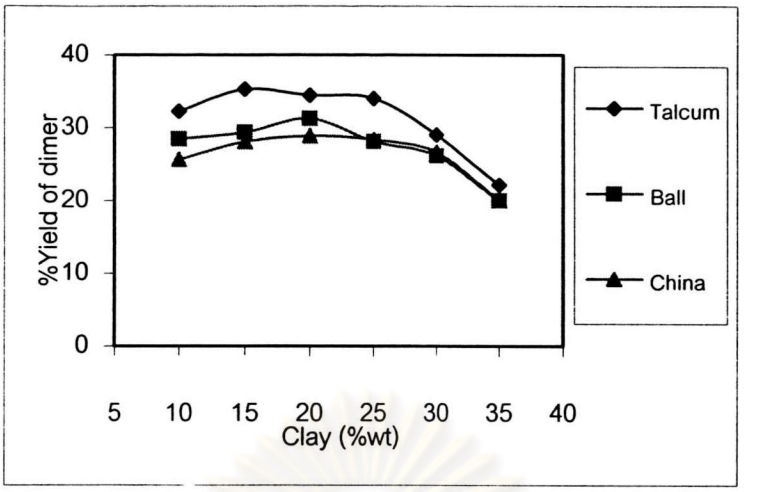

Figure 4.22 Effect of clay content on %yield of dimer at 60 ^{0}C, 24 hr., 0.05%wt cobalt naphthenate and 1.5%wt TBHP.

Under the optimum condition on dimerization of methyl oleate was 1.5%wt. TBHP, 0.05%wt cobalt naphthenate, 15%wt clay and 24 hr. at 60 ^{0}C. The product (Iodine Value = 96.74) obtained from dimerization reaction was yellow viscous liquid. Clays could be ranked according to the % dimerization as talcum (35.28%) > ball (31.27%) > china (28.89%) in Figure 4.22.

4.2.8.2 Characteristics of dimer obtained from methyl oleate using TBHP, cobalt naphthenate and clay as a catalyst at 60 ^{0}C

The IR spectra of methyl oleate and dimer are shown in Figures B9 and B28, respectively. The important absorption bands of methyl oleate and dimer are listed in Table 4.12.

Table 4.12 The IR absorption bands assignment of methyl oleate and dimer.

Wavenumber (cm^{-1})		Assignments
Methyl oleate	**Dimer**	
2851	2874	C-H Stretching, Aliphatic
1731	1735	C=O Stretching
1462	1467	C-H Bending, Aliphatic
1168	1163	C-O Stretching

The ^{1}H-NMR and ^{13}C-NMR spectra of methyl oleate and dimer are shown in Figures B10, B11, B29 and B30, respectively. Some signals of methyl oleate and dimer are shown in Table 4.13.

Table 4.13 The assignments of ^{1}H-NMR and ^{13}C-NMR spectra of methyl oleate and dimer using TBHP, cobalt naphthenate and clay as catalyst at 60 ^{0}C.

Position of Proton	Chemical Shift (δ, ppm)			
	Methyl oleate		Dimer	
	^{1}H	^{13}C	^{1}H	^{13}C
a	0.88	14.03	0.82	13.85
b	1.45	22.55	1.39	22.45
c	1.55	24.85	1.51	24.72
d	1.45	27.14	1.39	27.13
e	1.26	29.31	1.20	29.26
f	1.26	31.65	1.20	31.62
g	1.96	34.12	1.94	33.94
h	2.27	34.12	2.25	33.94
I	5.32	128.01,129.51	5.22	128.21,129.34
j	-	174.20	-	174.13
k	3.65	51.28	3.53	50.76
l	-	-	2.19	42.16
m	-	-	3.54	74.59

The molecular weight of dimer obtained from methyl oleate using TBHP, cobalt and clay as a catalyst at 60 ^{0}C was investigated using Matrix-assisted laser desorption/ionization mass spectrometry (MALDI-MS) with CCA as the matrix. The result was shown in figure 4.23.

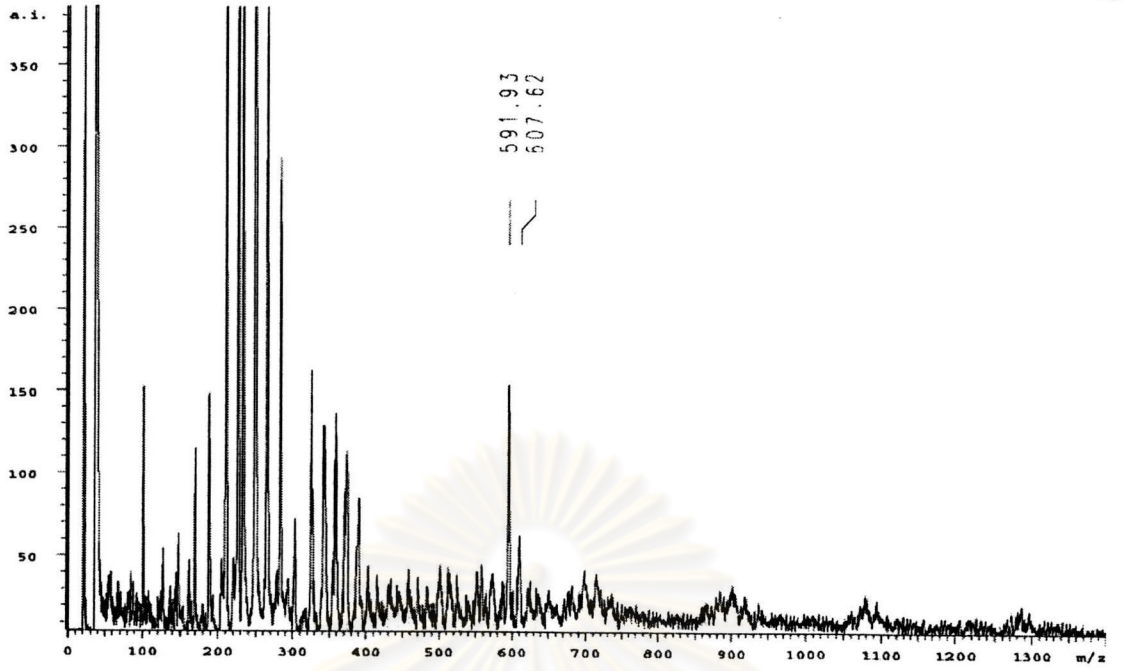

Figure 4.23 MALDI spectrum of dimer obtained from methyl oleate using TBHP, cobalt naphthenate and clay as a catalyst at 60 ^{0}C.

The chemical equation of the reaction was represented as in Figure 4.24.

Figure 4.24 The proposed structure of dimer obtained from methyl oleate using TBHP, cobalt naphthenate and clay as a catalyst at 60 ^{0}C.

Mechanism of dimerization of methyl oleate by free radical is shown in 4.2.4.4 From the results of table 4.13, it could be concluded that the product was dimer and its structure was as follows:

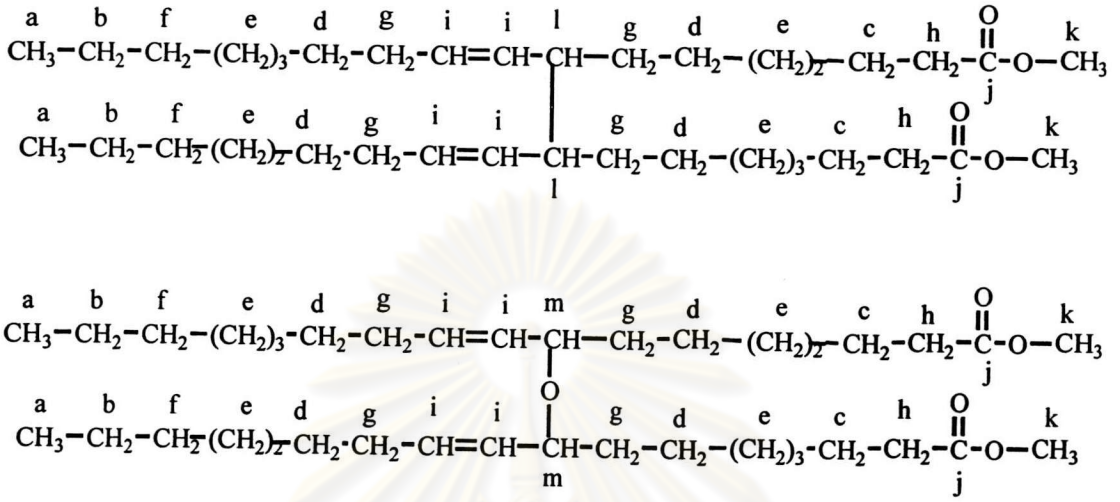

Dimerization of methyl oleate using clay catalyst at 230-270 ^{0}C produced a dimer containing carbon linkage (C-C) were identified by NMR (Table 4.5) and MALDI-MS (MW. 594). The optimum condition for dimerization of methyl oleate was 25%wt clay at 250 ^{0}C for 4 hr. Talcum (17.20%) showed higher percent dimerization than ball clay (12.55%) and china clay (10.47%), respectively. However, its dimerization was not good, therefore, dimerization of methyl oleate using cobalt naphthenate as catalyst and tert-butylhydroperoxide as cocatalyst was studied. At room temperature, free radical dimerization was done under a vigorous stream of air producing dimers with peroxide linkage (C-O-O-C) were identified by NMR (Table 4.7) and MALDI-MS (MW.623), with 44.45%wt of dimer formation. In contrast, after increasing the reaction temperature to 60 ^{0}C, the dimer fraction from methyl oleate contained no peroxide linkage, whereas its with carbon linkage were identified by NMR (Table 4.9) and MALDI-MS (MW. 591) because the peroxide linkage was readily cleaved thermally, so that, the suitable condition for dimerization of methyl oleate is observed at 60 ^{0}C for 24 hr., using 15%wt clay, 0.05%wt cobalt naphthenate

and 1.5%wt *tert*-butylhydroperoxide. At this condition the dimer (35.28%) contained carbon linkage were identified by NMR (Table 4.9) and MALDI-MS (MW.591). It was found that dimer formation was better than those using only clay. However, its dimerization was less than using coabalt naphthenate and TBHP catalyst.

In this study, the dimer formation can be characterized for their molecular weight by MALDI-MS. It was found that free radical mechanism dimerization of methyl oleate using 0.05 %wt cobalt naphthenate, 1.5%wt TBHP and 15%wt clay could be done at mild condition (60 ^{0}C, 24 hr.) and gave 44.28% yield of dimer, which dimerization using acid activated talcum at 250 ^{0}C for 4 hr. gave only 17.20% yield of dimer. Moreover, dimers obtained from clay catalyst and cobalt naphthenate catalyst were different as revealed by the molecular weight of the major dimer products. The carbon-carbon linked dimer was obtained in the clay catalyzed dimerization process, while dimers containing carbon-oxygen linkage were obtained from cobalt naphthenate/oxygen dimerization process. Comparing with literature [31] reported process of dimerization fatty acids from monounsaturated at 230-260 ^{0}C, 3-4 hours using 1-20 % montmorillonite clay as catalyst. The product have 60% carbon-carbon linked dimer.

CHAPTER V

CONCLUSION AND SUGGESTION

5.1 Conclusion

The dimerization of methyl oleate was carried out using 25%wt acid activated clays at 250 ^{0}C for 4 hours. At this condition, talcum showed higher % of carbon-carbon dimer of methyl oleate than the other clay samples. From this condition, clays could be ranked according to the % dimerization as talcum (17.20%) > ball (12.55%) > china (10.47%).

Dimerization of methyl oleate using 0.05%wt cobalt naphthenate at room temperature for 120 hours, gave 44.45% of peroxide linkage dimer. However, at 60 ^{0}C for 48 hours, 35.55% of the carbon-carbon dimer was obtained.

Dimerization of methyl oleate using 0.07%wt cobalt naphthenate and 1.5%wt *tert*-butylhydroperoxide at room temperature for 72 hours gave 66.09% of dimer containing peroxide linkage. However, at 60 ^{0}C for 24 hours, the carbon-carbon dimer (44.28%) was obtained.

The dimerization of methyl oleate using 0.05%wt cobalt naphthenate, 1.5%wt *tert*-butylhydroperoxide, and 15%wt clay at 60 ^{0}C for 24 hours gave a mixture of dimers. At this condition, talcum showed higher carbon-carbon linked dimer formation (35.28%) than did other clays.

The identity of dimer was characterized by IR, ^{1}H-NMR, ^{13}C-NMR and MALDI-MS and the spectroscopic data were as expected for each dimer. The summary of reaction condition were shown in Table 5.1.

Table 5.1 The optimum condition and %yield of dimers for dimerization of methyl oleate using various catalyst.

Catalyst	Optimum condition			Dimers (%yield)	
	Content (%wt.)	Time (hr.)	Temp. (^{0}C)	C-C	C-O-O-C
Clay	25	4	250	17.2	-
Cobalt naphthenate	0.05	120	room temp.	-	44.45
Cobalt naphthenate	0.05	48	60	35.55	-
Cobalt naphthenate, TBHP	0.07, 1.5	72	room temp.	-	66.09
Cobalt naphthenate, TBHP	0.05, 1.5	24	60	44.28	-
Cobalt naphthenate, TBHP, Clay	15, 0.05, 1.5	24	60	35.28	-

5.2 Suggestions for future work

1. Dimerization of methyl oleate at high temperature and high pressure should be investigated.
2. Application of this method to other unsaturated fatty acid should be investigated.